Double Higgs Production at HL-LHC

K.C. Kong
University of Kansas

2021 Chung-Ang University Beyond the Standard Model Workshop

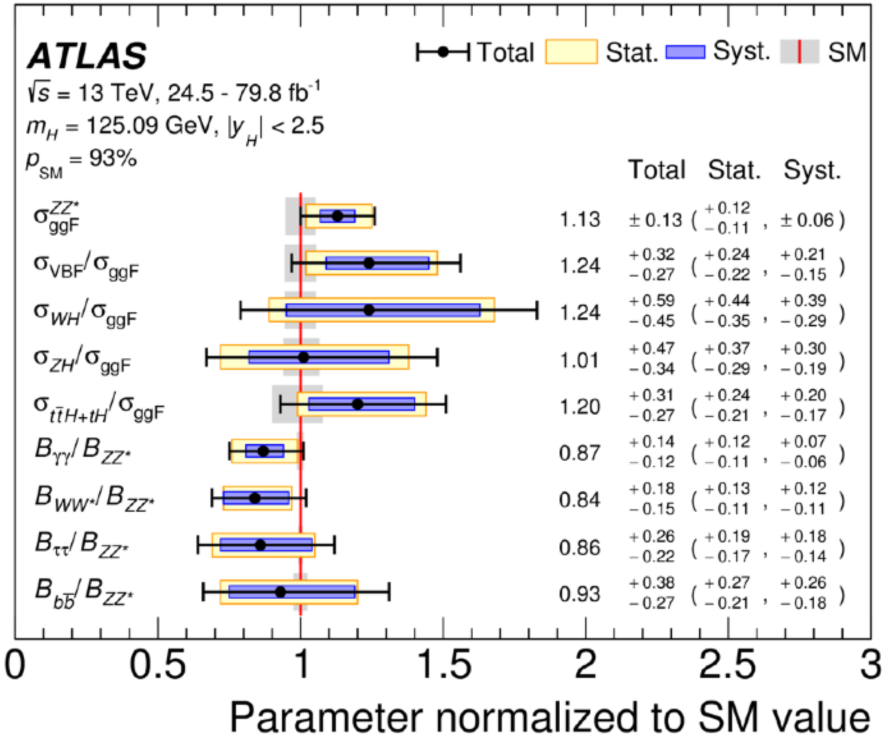

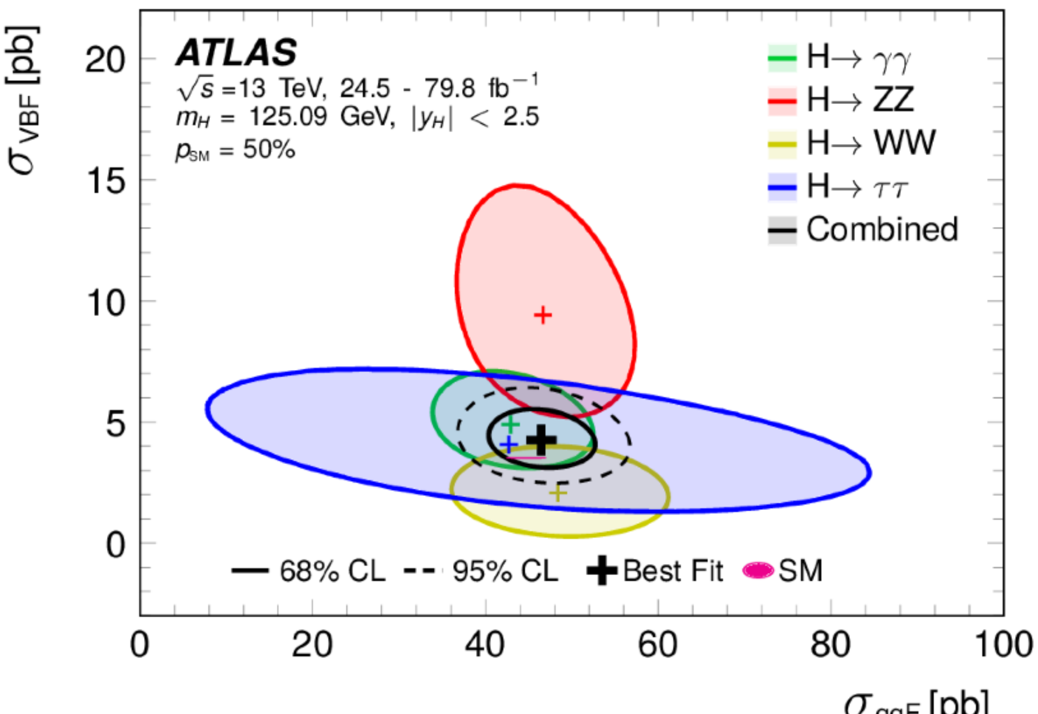

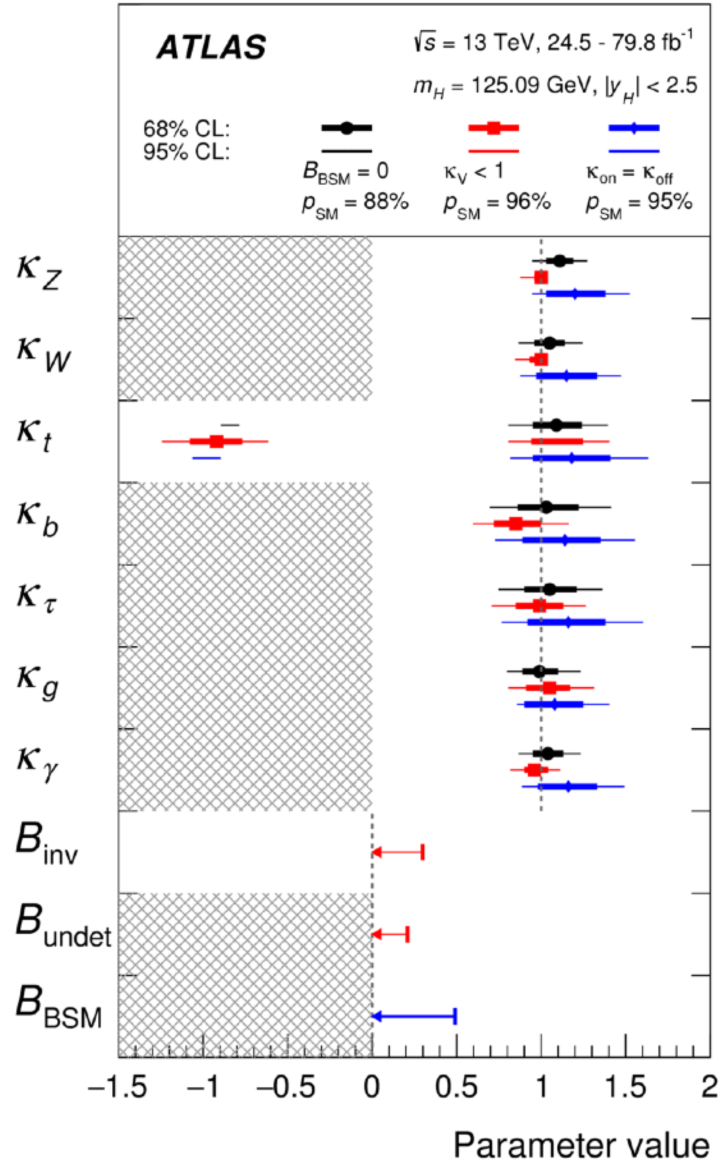

- Observed Higgs couplings appear to be consistent with SM prediction.
- Apart from precision measurement of mass, spin, couplings to SM particles, what is left?

Why double Higgs (hh) ?

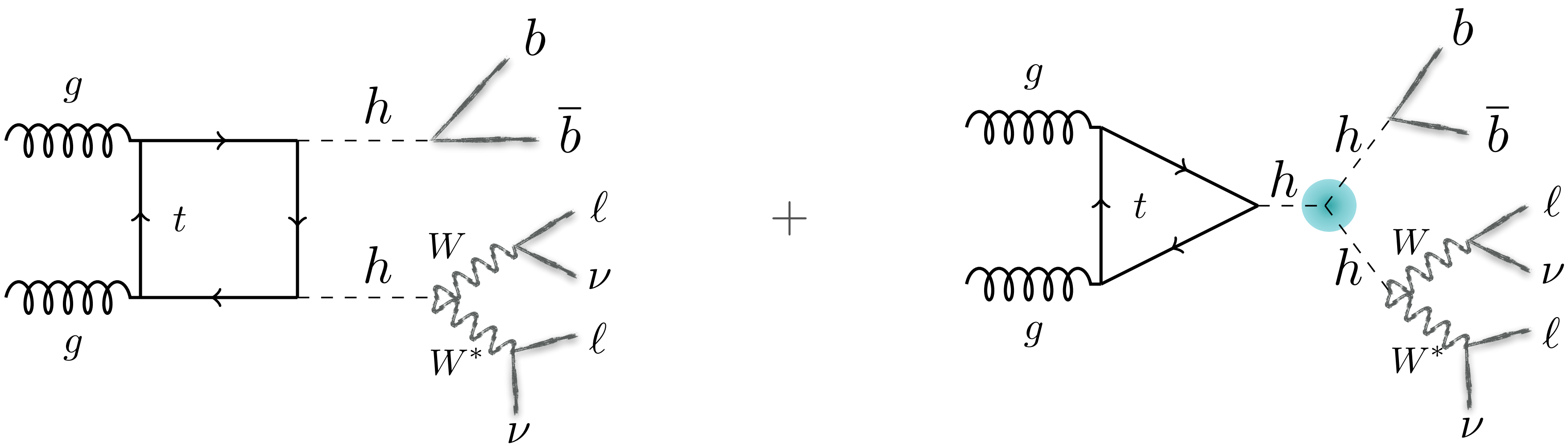

$$V_h = \frac{m_h^2}{2} h^2 + c_3 \frac{m_h^2}{2v} h^3 + c_4 \frac{m_h^2}{8v^2} h^4$$

$$\sim c_3 y_t^2 \frac{\alpha_S}{4\pi} \frac{m_h^2}{\hat{s}} \left(log \frac{m_t^2}{\hat{s}} + i\pi \right)^2$$

- Measurement of triple and quartic couplings provides crucial input to confirm SM prediction. The knowledge of c3 and c4 is crucial to reconstruct the Higgs potential for better understanding of EWSB. Any deviation will lead to new physics beyond SM. The HL-LHC will have opportunity to probe triple Higgs self-coupling (c_3), while we will need a new machine to probe quartic coupling (c4).
- The c_3 is sensitive at lower-energy bins where the backgrounds are large.
- Destructive interference between two diagrams in SM makes it difficult to probe c3.

Why double Higgs (*hh*) ?

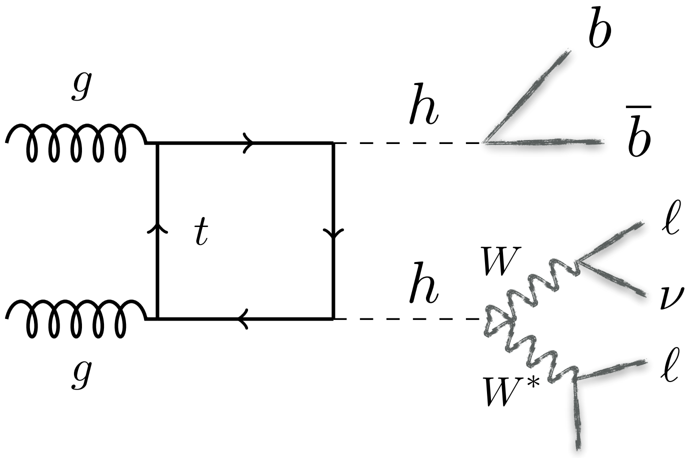

+

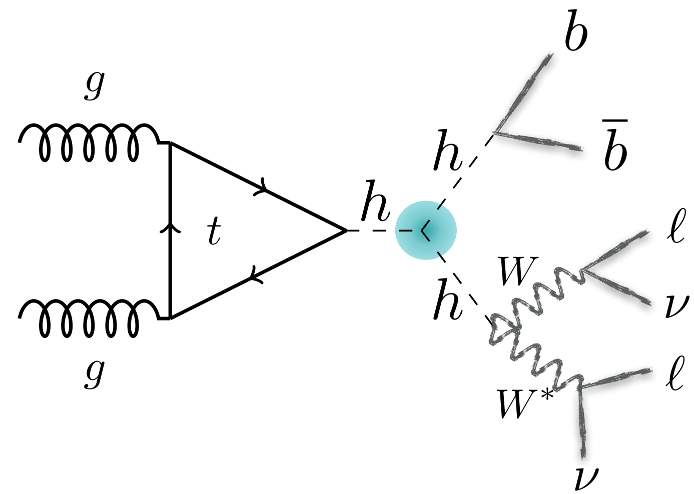

$$\sim c_3 y_t^2 \frac{\alpha_S}{4\pi} \frac{m_h^2}{\hat{s}} \left(log \frac{m_t^2}{\hat{s}} + i\pi \right)^2$$

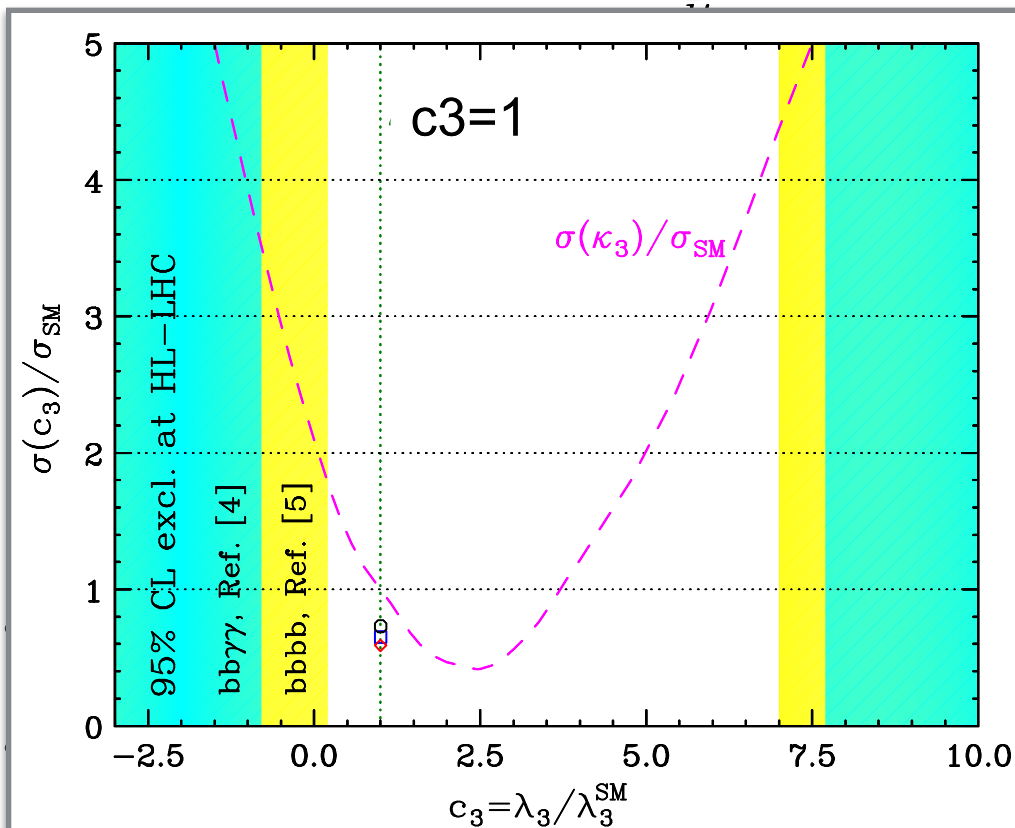

des crucial input to confirm SM prediction. The
e Higgs potential for better understanding of EWSB.
I. The HL-LHC will have opportunity to probe triple
machine to probe quartic coupling (c4).

e the backgrounds are large.

ms in SM makes it difficult to probe c3.

Double Higgs Production

- Resonant / non-resonant double Higgs production is interesting, theoretically and experimentally.
  - It is a guaranteed physics at HL-LHC with high impact.
  - It is challenging experimentally.
  - Triple Higgs coupling is easily modified in many extensions of SM.
  - Double Higgs production provides measurement of the first non-trivial term (cubic term) in the Higgs potential.
  - It brings many different final states.

	bb	WW^*	$\tau\tau$	ZZ^*	$\gamma\gamma$
bb	33%				
WW^*	25%	4.6%			
$\tau\tau$	7.3%	2.7%	0.39%		
ZZ^*	3.1%	1.1%	0.33%	0.069%	
$\gamma\gamma$	0.26%	0.1%	0.028%	0.012%	0.0005%

Decays

$\sigma(hh)^{NNLO}_{SM} \simeq 40.7$ fb (14 TeV)

higher branching ratios

cleaner final state

	bb	WW^*	$\tau\tau$	ZZ^*	$\gamma\gamma$
bb	33%				
WW^*	25%	4.6%			
$\tau\tau$	7.3%	2.7%	0.39%		
ZZ^*	3.1%	1.1%	0.33%	0.069%	
$\gamma\gamma$	0.26%	0.1%	0.028%	0.012%	0.0005%

1902.00134	Statistical-only ATLAS	Statistical-only CMS	Statistical + Systematic ATLAS	Statistical + Systematic CMS
$HH \to b\bar{b}b\bar{b}$	1.4	1.2	0.61	0.95
$HH \to b\bar{b}\tau\tau$	2.5	1.6	2.1	1.4
$HH \to b\bar{b}\gamma\gamma$	2.1	1.8	2.0	1.8
$HH \to b\bar{b}VV(ll\nu\nu)$	-	0.59	-	0.56
$HH \to bbZZ(4l)$	-	0.37	-	0.37
combined	3.5	2.8	3.0	2.6
	Combined 4.5		Combined 4.0	

4σ expected for ATLAS+CMS!

- These measurements are challenged by a low σ (hh) and small branching ratios (BR).
- No single channel is expected to reach 3 sigma at HL-LHC.
- The combination of different channels is crucial. bbWW has good potential for further improvement.

Experimental status on c_3 @ LHC 13 TeV

CMS PAS HIG-17-030

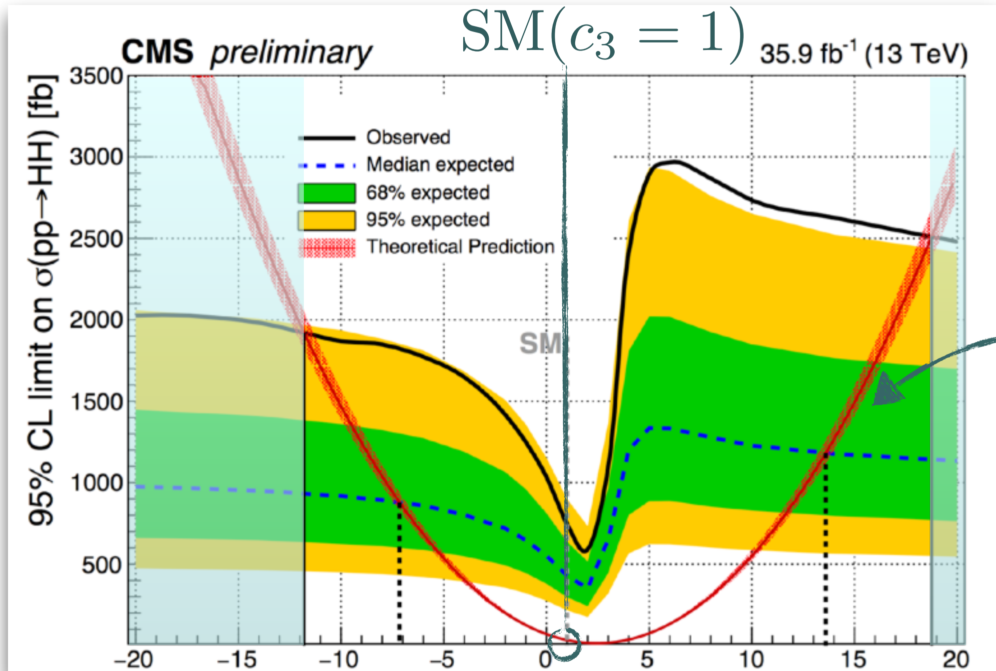

c_3

- Allowed region of c_3.

$$-11.8 < c_3 < 18.8$$

$$(b\bar{b}\gamma\gamma \; + \; b\bar{b}\tau\tau + \; b\bar{b}b\bar{b} \; + \; b\bar{b}VV)$$

$$\frac{\sigma}{\sigma_{SM}} = A_1\, c_t^4 + A_3\, c_t^2 c_3^2 + A_7\, c_t^3 c_3$$

- Allowed range of hh cross sections.

$$\sigma_{hh}^{observed} / \sigma_{hh}^{SM} = 22$$

- The $bb\gamma\gamma$ and $bb\tau\tau$ are leading channels.

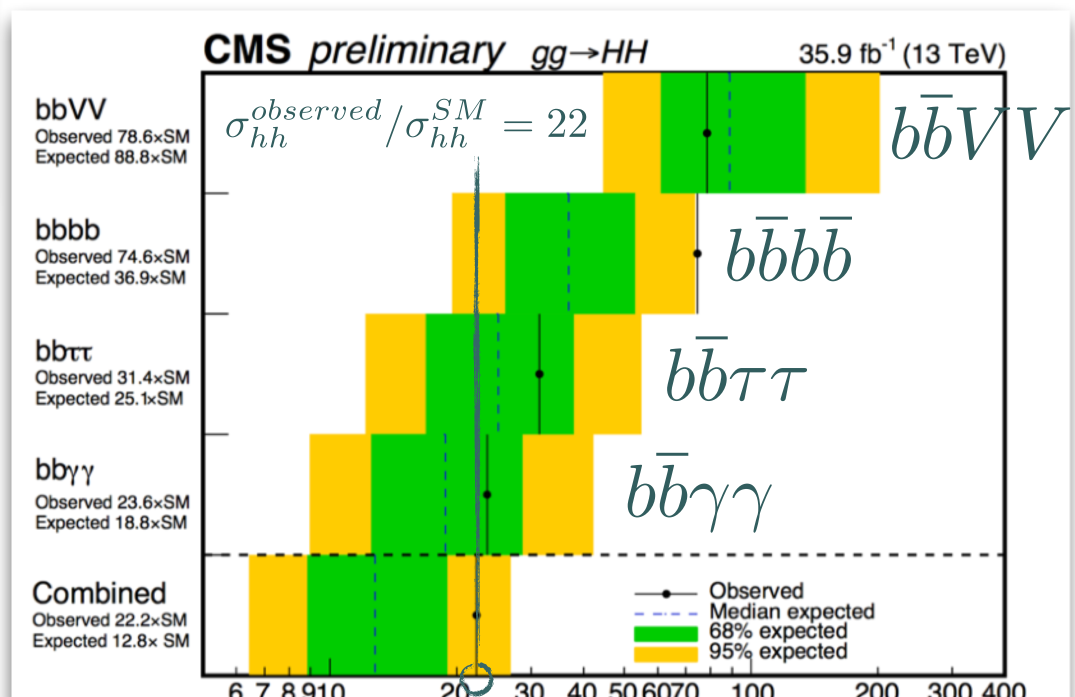

$95\%\ CL\ on\ \sigma_{hh}/\sigma_{hh}^{SM}$

Recent CMS analysis

DNN
1708.04188

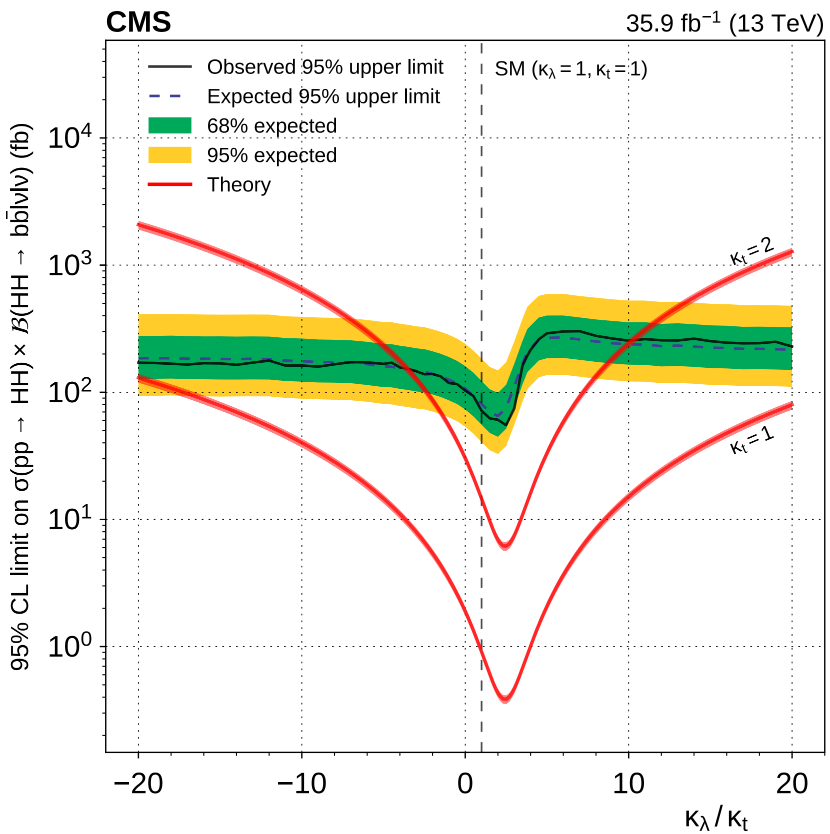

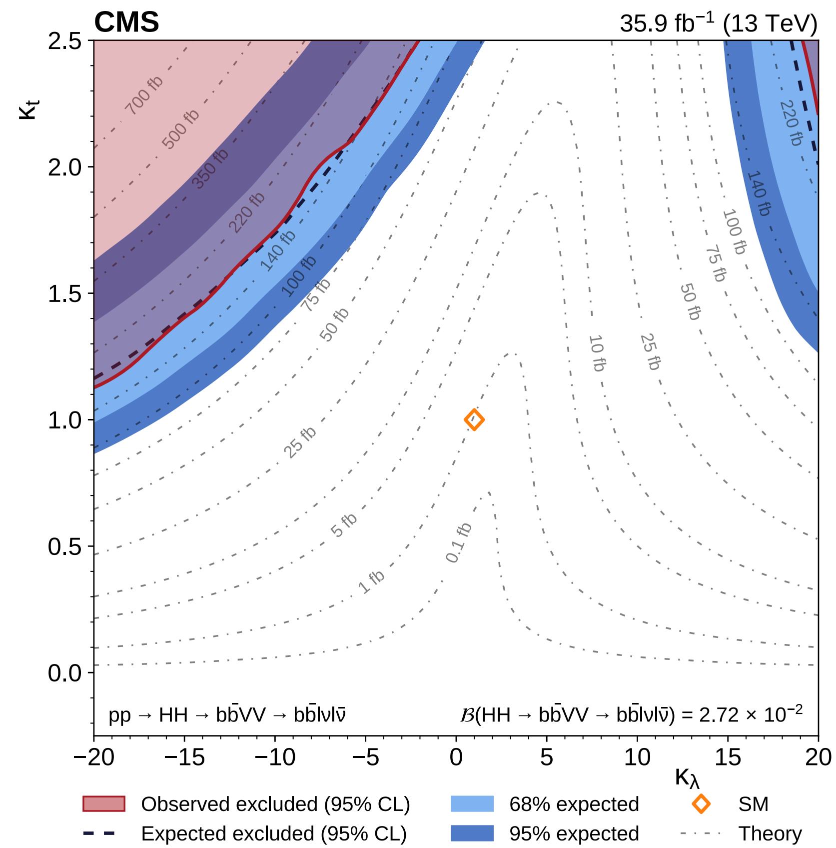

$m_{\ell\ell}$

$\Delta R_{\ell\ell}$

ΔR_{jj}

$\Delta\phi(\ell\ell, jj)$

$p_T^{\ell\ell}$

p_T^{jj}

$\min(\Delta R_{j\ell})$

m_T

Searches for resonant and nonresonant pair-produced Higgs bosons (HH) decaying respectively into $\ell\nu\ell\nu$, through either W or Z bosons, and $b\bar{b}$ are presented. The analyses are based on a sample of proton-proton collisions at $\sqrt{s} = 13$ TeV, collected by the CMS experiment at the LHC, corresponding to an integrated luminosity of 35.9 fb^{-1}. Data and predictions from the standard model are in agreement within uncertainties. For the standard model HH hypothesis, the data exclude at 95% confidence level a product of the production cross section and branching fraction larger than 72 fb, corresponding to 79 times the standard model prediction.

Combination results: non-resonant production

1906.02025

HH production cross-section:

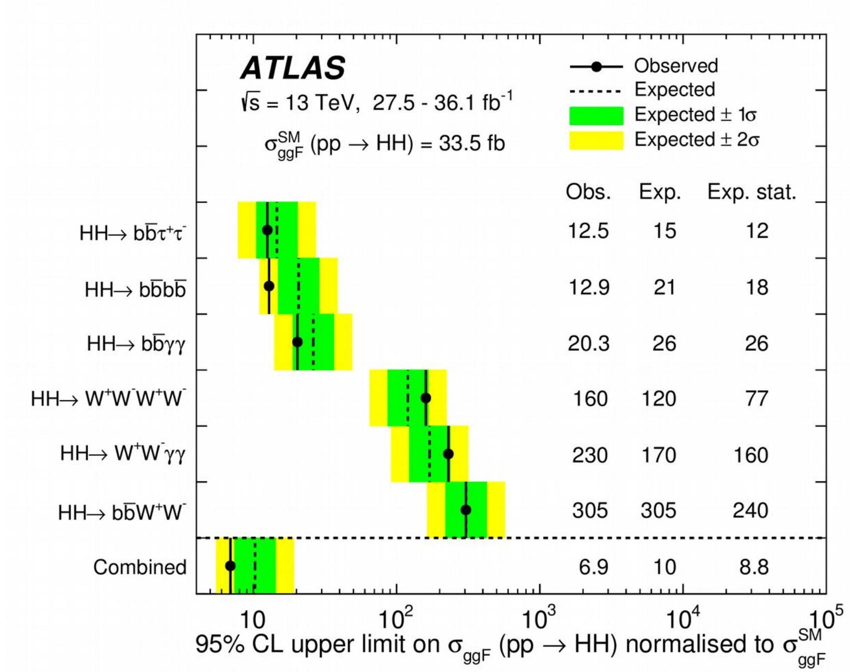

Higgs trilinear coupling:

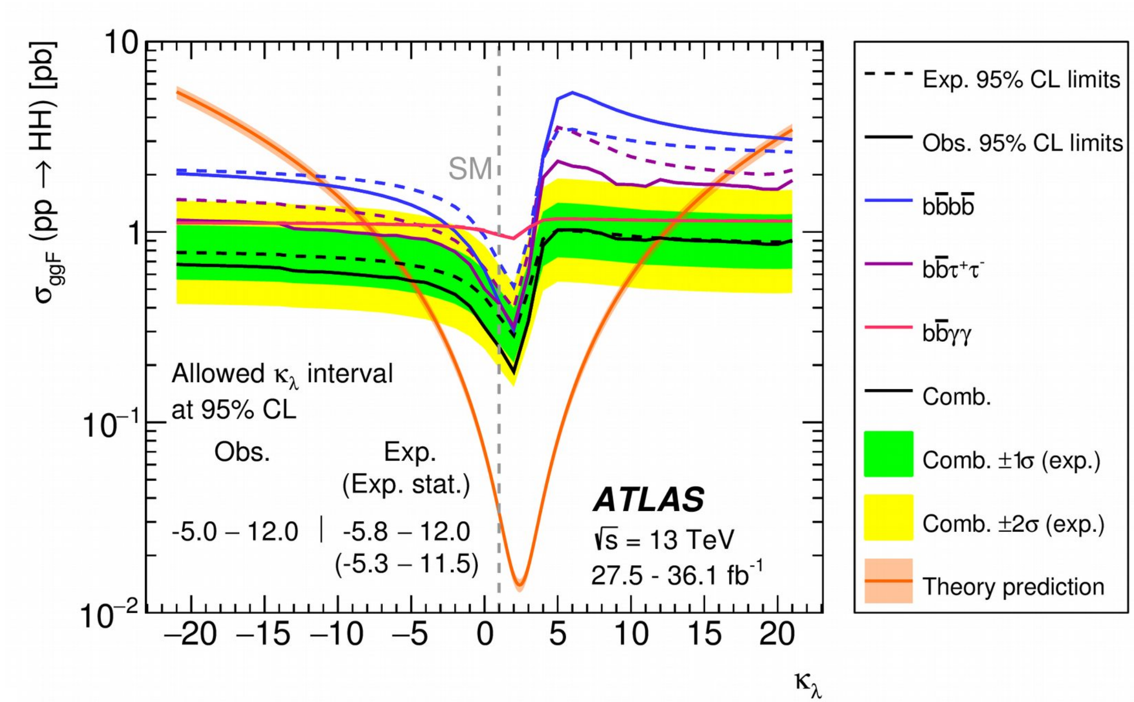

95% CL upper limit for $k_\lambda \equiv \frac{\lambda_{HHH}}{\lambda_{HHH}^{SM}} = 1$:

- 6.9 x $\sigma_{ggF}^{\mathrm{SM}}$ (obs)
- 10.0 x $\sigma_{ggF}^{\mathrm{SM}}$ (exp)

no study for non-resonant hh -> bbWW* in the dilepton channel.

95% CL confidence intervals:

- Kλ ∈ [-5.0,12] (obs), [-5.8,12] (exp)

ATL-PHYS-PUB-2019-009

- Indirect limits from single Higgs differential production and decay measurement (80fb^{-1}):
  - Kλ ∈ [-3.2,11.9] (obs), [-5.8,12.0] (exp)

Experimental status on c_3 @ LHC 13 TeV

$27.5 - 36.1\ \mathrm{fb}^{-1} (13\ \mathrm{TeV})$

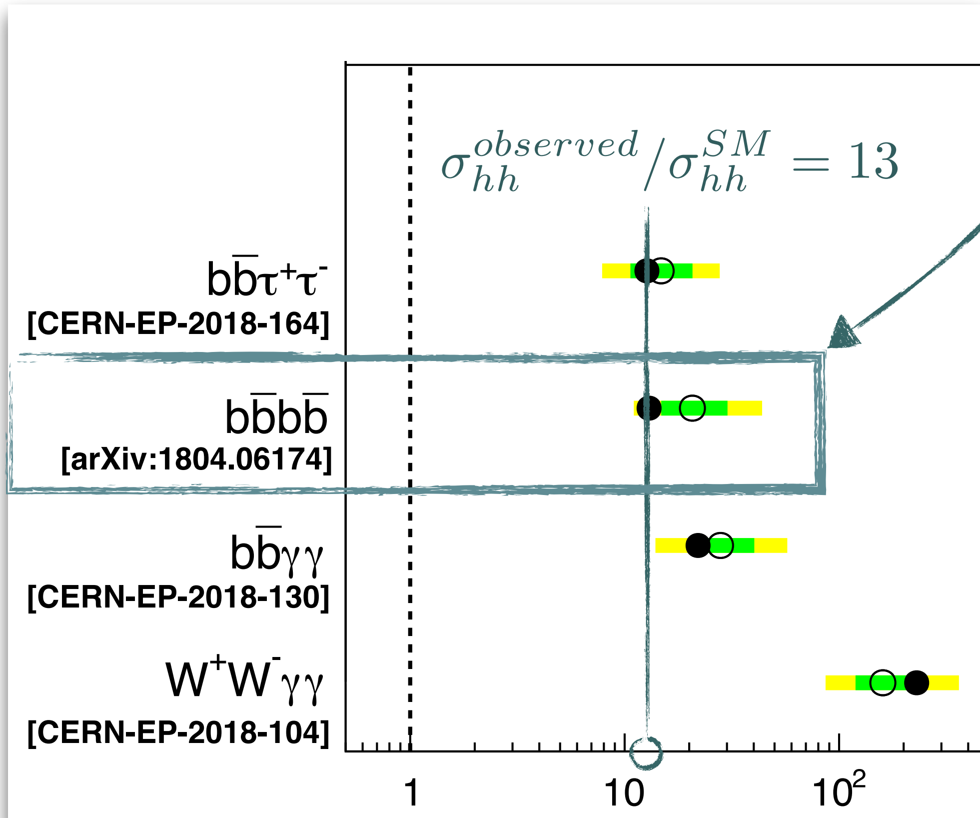

$95\%\ CL\ on\ \sigma_{hh}/\sigma_{hh}^{SM}$

ATLAS, PRL 117 (2016) 079901

ATLAS, PRL 117 (2016) 012001

- The *bbbb* channel is significantly improved!
- Using an improved *b*-tagging algorithm (*MV2c10*)

$$\epsilon_b = 70\ \%$$
$$\epsilon_{c\to b} = 8.3 \sim 14.1\ \%$$
$$\epsilon_{j\to b} = 0.26 \sim 0.83\ \%$$

- Allowed region of c_3.

$$-8.2 \lesssim c_3 \lesssim 13.2 \quad (\text{Using only } b\bar{b}\gamma\gamma)$$

Recent ATLAS analysis

1908.06765

Table 2: Description of the variables used as inputs to the DNN classifier.

(p_T, η, ϕ)	p_T, η, and ϕ of the leptons, leading two signal jets, and leading two b-tagged jets
Dilepton flavour	Whether the event is composed of two electrons, two muons, or one of each
$\Delta R_{\ell\ell}$, $\lvert\Delta\phi_{\ell\ell}\rvert$	ΔR and magnitude of the $\Delta\phi$ between the two leptons
$m_{\ell\ell}$, $p_T^{\ell\ell}$	Invariant mass and the transverse momentum of the dilepton system
$E_{\mathrm{T}}^{\mathrm{miss}}$, $E_{\mathrm{T}}^{\mathrm{miss}}$-$\phi$	Magnitude of the missing transverse momentum vector and its ϕ component
$\lvert\Delta\phi(\mathbf{p}_{\mathrm{T}}^{\mathrm{miss}}, \mathbf{p}_{\mathrm{T}}^{\ell\ell})\rvert$	Magnitude of the $\Delta\phi$ between the $\mathbf{p}_{\mathrm{T}}^{\mathrm{miss}}$ and the transverse momentum of the dilepton system
$\lvert\mathbf{p}_{\mathrm{T}}^{\mathrm{miss}} + \mathbf{p}_{\mathrm{T}}^{\ell\ell}\rvert$	Magnitude of the vector sum of the $\mathbf{p}_{\mathrm{T}}^{\mathrm{miss}}$ and the transverse momentum of the dilepton system
Jet multiplicities	Numbers of b-tagged and non-b-tagged jets
$\lvert\Delta\phi_{bb}\rvert$	Magnitude of the $\Delta\phi$ between the leading two b-tagged jets
m_{T2}^{bb}	m_{T2} [119] using the leading two b-tagged jets as the visible inputs and $\mathbf{p}_{\mathrm{T}}^{\mathrm{miss}}$ as invisible input
H_{T2}	Scalar sum of the magnitudes of the momenta of the $H \to \ell\nu\ell\nu$ and $H \to bb$ systems, $$H_{\mathrm{T2}} = \lvert\mathbf{p}_{\mathrm{T}}^{\mathrm{miss}} + \mathbf{p}_{\mathrm{T}}^{\ell,0} + \mathbf{p}_{\mathrm{T}}^{\ell,1}\rvert + \lvert\mathbf{p}_{\mathrm{T}}^{b,0} + \mathbf{p}_{\mathrm{T}}^{b,1}\rvert$$
$H_{\mathrm{T2}}^{\mathrm{R}}$	Ratio of H_{T2} and scalar sum of the transverse momenta of the H decay products, $$H_{\mathrm{T2}}^{\mathrm{R}} = H_{\mathrm{T2}}/(E_{\mathrm{T}}^{\mathrm{miss}} + \lvert\mathbf{p}_{\mathrm{T}}^{\ell,0}\rvert + \lvert\mathbf{p}_{\mathrm{T}}^{\ell,1}\rvert + \lvert\mathbf{p}_{\mathrm{T}}^{b,0}\rvert + \lvert\mathbf{p}_{\mathrm{T}}^{b,1}\rvert),$$ where $\mathbf{p}_{\mathrm{T}}^{\ell(b),0\{1\}}$ are the transverse momenta of the leading {subleading} lepton (b-tagged jet)

- DNN: two fully connected laters with 250 neurons and ReLu,
- One dropout layer between the two
- Four outputs $p_i \ (i \in \{HH, \mathrm{Top}, \mathrm{Z}\text{-}\ell\ell, \mathrm{Z}\text{-}\tau\tau\})$ $d_{HH} = \ln\left[p_{HH}/\left(p_{\mathrm{Top}} + p_{\mathrm{Z}\text{-}\ell\ell} + p_{\mathrm{Z}\text{-}\tau\tau}\right)\right]$

Recent ATLAS analysis

A search for non-resonant Higgs boson pair production, as predicted by the Standard Model, is presented, where one of the Higgs bosons decays via the $H \to bb$ channel and the other via one of the $H \to WW^*/ZZ^*/\tau\tau$ channels. The analysis selection requires events to have at least two b-tagged jets and exactly two leptons (electrons or muons) with opposite electric charge in the final state. Candidate events consistent with Higgs boson pair production are selected using a multi-class neural network discriminant. The analysis uses 139 fb^{-1} of pp collision data recorded at a centre-of-mass energy of 13 TeV by the ATLAS detector at the Large Hadron Collider. An observed (expected) upper limit of 1.2 ($0.9^{+0.4}_{-0.3}$) pb is set on the non-resonant Higgs boson pair production cross-section at 95% confidence level, which is equivalent to 40 (29^{+14}_{-9}) times the value predicted in the Standard Model.

	-2σ	-1σ	**Expected**	$+1\sigma$	$+2\sigma$	**Observed**
$\sigma\,(gg \to HH)$ [pb]	0.5	0.6	0.9	1.3	1.9	1.2
$\sigma\,(gg \to HH)\,/\sigma^{\text{SM}}\,(gg \to HH)$	14	20	29	43	62	40

1908.06765

Previously on $hh \to bbWW^*$

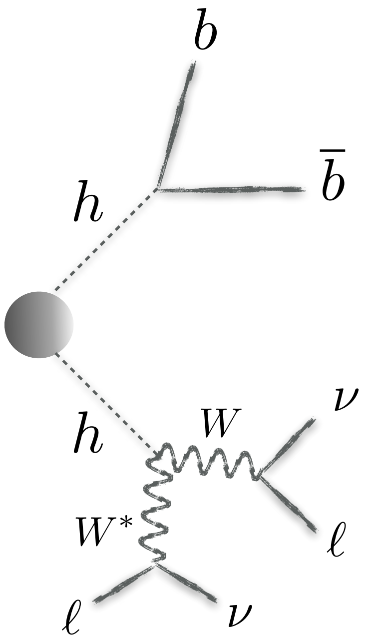

Signal

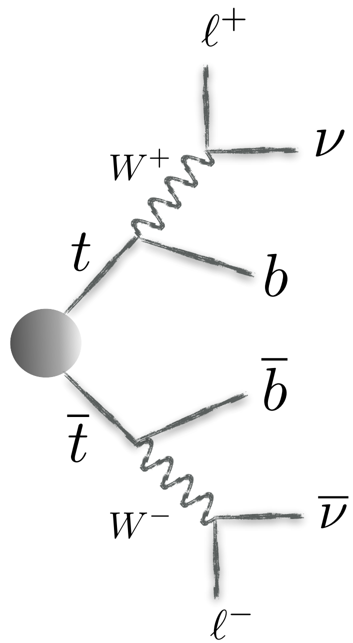

Major background

- $hh \to bbWW^*$ channel suffers from the large $t\bar{t}$ background.
- The sensitivity of signal in the di-leptonic mode is very poor.

CMS-FTR-15-002-PAS

Adhikary, Banerjee, Barman, Bhattacherjee, Niyogi 2017

- The situation in the semi-leptonic mode is even worse…

Dolan, Englert, Spannowsky 2012

Adhikary, Banerjee, Barman, Bhattacherjee, Niyogi 2017

cf) Papaefstathiou, Yang, Zurita 2012

Seemingly it looks hopeless…

hh → bbWW: dilepton channel*

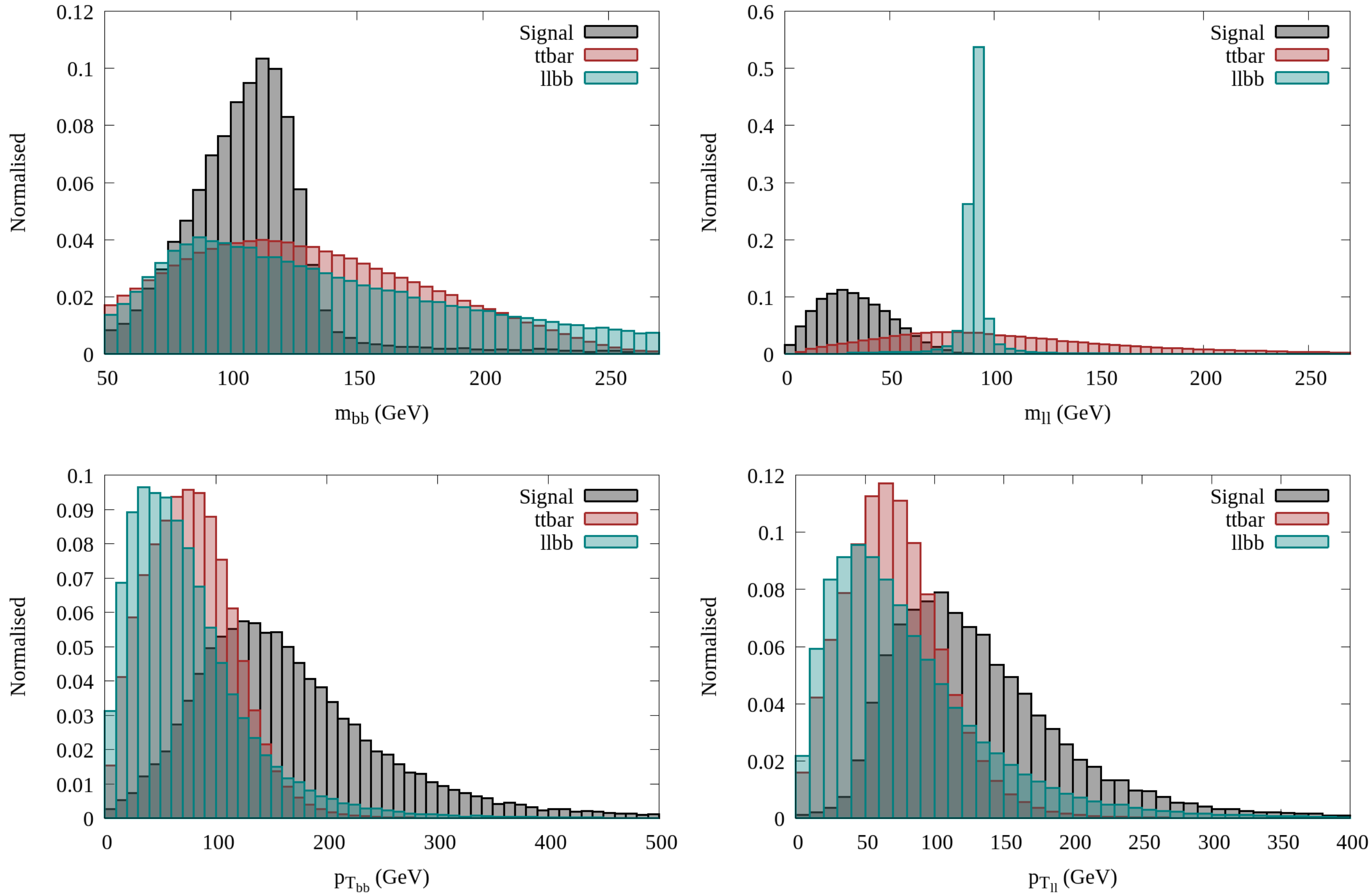

10 variables: $p_{T,\ell_{1/2}},\ \not{E}_T,\ m_{\ell\ell},\ m_{bb},\ \Delta R_{\ell\ell},\ \Delta R_{bb},\ p_{T,bb},\ p_{T,\ell\ell},\ \Delta\phi_{bb\ \ell\ell}$

Adhikary, Banerjee, Barman, Bhattacherjee, Niyogi 2017

$hh \to bbWW^*$: dilepton channel

HL-LHC, 14 TeV, L=3 ab^{-1}

Adhikary, Banerjee, Barman, Bhattacherjee, Niyogi JHEP 2017

$\not{E}_T$

$p_{T,\ell_{1/2}}$ $\Delta\phi_{bb\,\ell\ell}$

$\Delta R_{\ell\ell}$ ΔR_{bb}

m_{bb} $m_{\ell\ell}$

$p_{T,bb}$ $p_{T,\ell\ell}$

Sl. No.	Process	Order	Events
Background	$t\bar{t}$ lep	NNLO [128]	2080.52
	$t\bar{t}h$	NLO [111]	131.66
	$t\bar{t}Z$	NLO [130]	106.31
	$t\bar{t}W$	NLO [129]	35.97
	$hb\bar{b}$	NNLO (5FS) + NLO (4FS) [111]	~ 0
	$\ell\ell b\bar{b}$	LO	842.72
	Total		3197.18
Signal ($hh \to b\bar{b}WW \to b\bar{b}\ell\ell + \not{E}_T$)		NNLO [70]	35.20
Significance ($S/\sqrt{B}$)			0.62

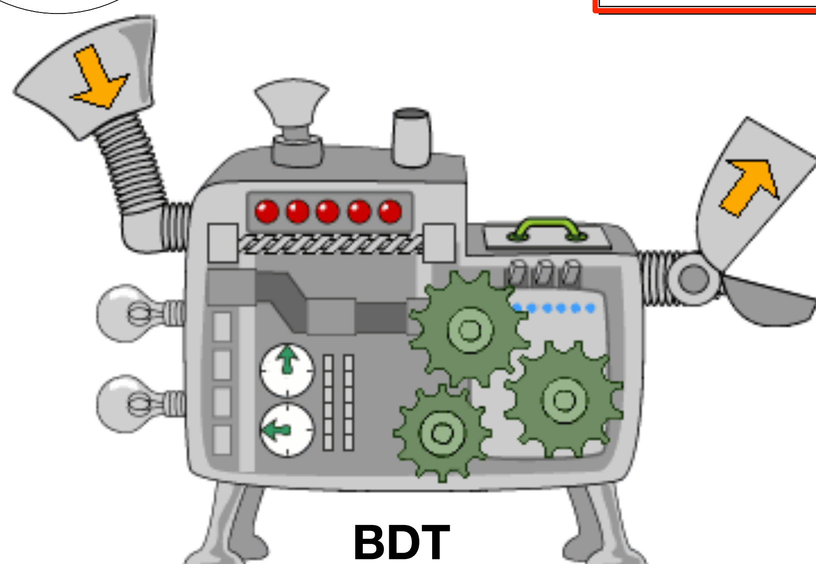

~ dN/dsqrt(s)

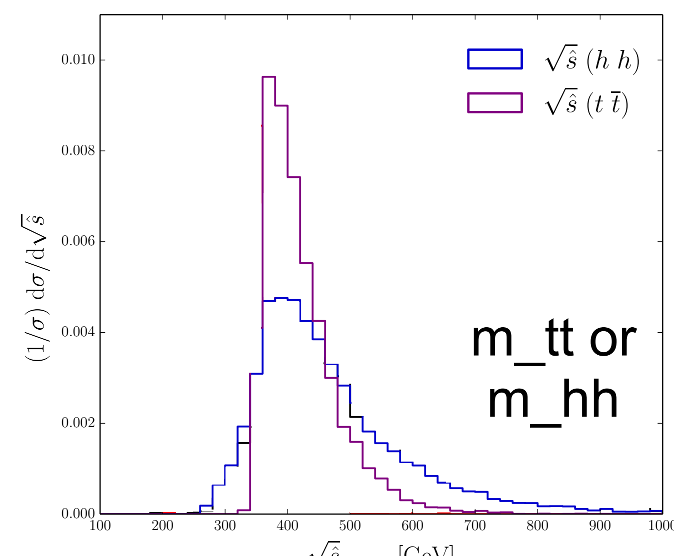

$hh \to bbWW^*$: dilepton channel

HL-LHC, 14 TeV, L=3 ab^{-1}

Adhikary, Banerjee, Barman, Bhattacherjee, Niyogi JHEP 2017

Sl. No.	Process	Order	Events
Background	$t\bar{t}$ lep	NNLO [128]	2080.52
	$t\bar{t}h$	NLO [111]	131.66
	$t\bar{t}Z$	NLO [130]	106.31
	$t\bar{t}W$	NLO [129]	35.97
			~ 0
			842.72
			3197.18
Signal ($hh \to$			35.20
			0.62

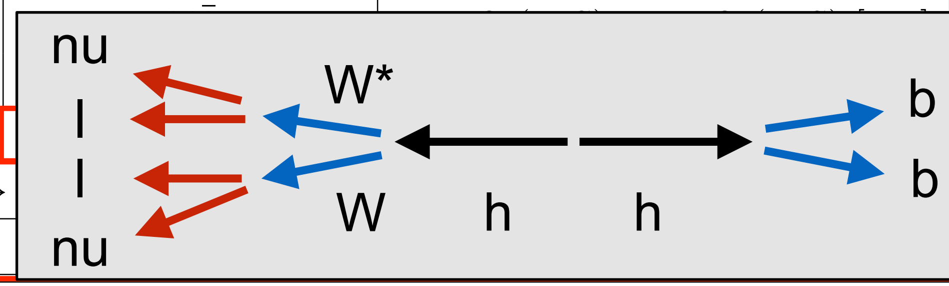

$\not{E}_T$

$p_{T,\ell_{1/2}}$ $\Delta\phi_{bb\ \ell\ell}$

$\Delta R_{\ell\ell}$ ΔR_{bb}

m_{bb} $m_{\ell\ell}$

$p_{T,bb}$ $p_{T,\ell\ell}$

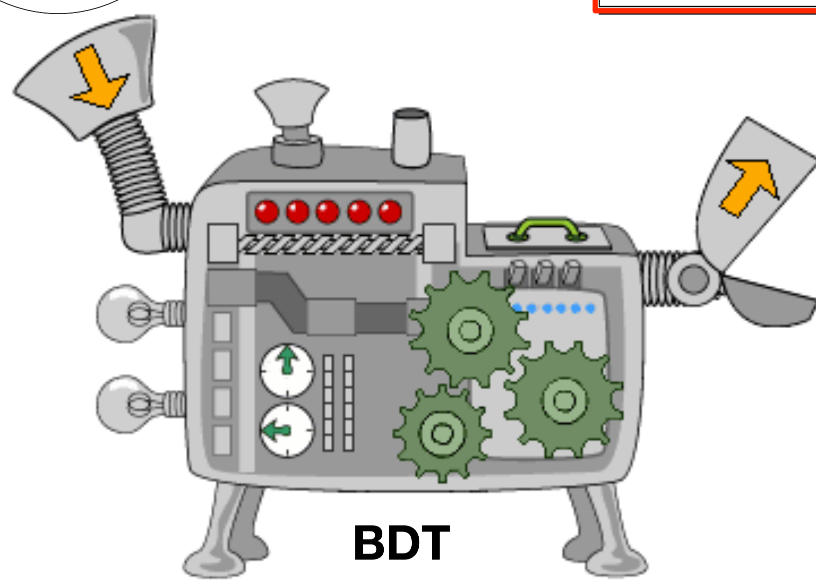

~ dN/dsqrt(s)

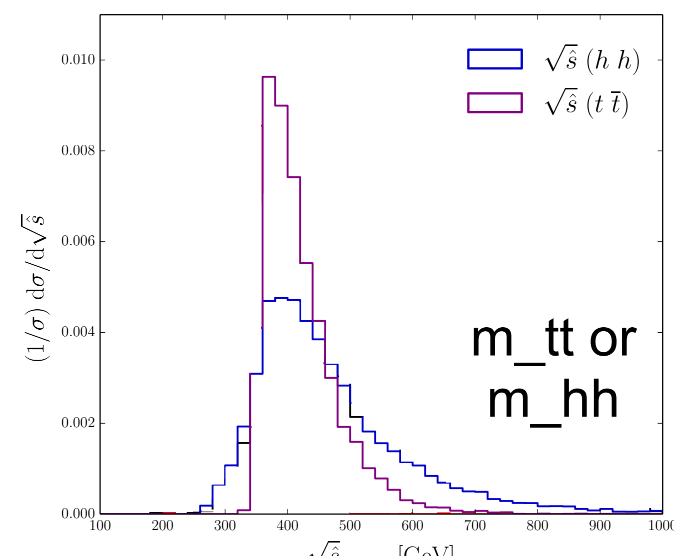

Cross sections @14 TeV LHC

Kim, Kong, Matchev, Park, PRL 2019

$\sigma_{hh} = 40.7\ \text{fb}$ (NNLO)

$\sigma_{hh} \cdot 2 \cdot \text{BR}(h \to b\bar{b}) \cdot \text{BR}(h \to WW^* \to \ell^+\ell^-\nu\bar{\nu}) = 0.648\,\text{fb}$

ℓ denotes an electron or a muon, including leptons from tau decays.

- tt: 953.6 pb (NNLO)
- tth: 611.3 fb (NLO)
- ttV (V=W, Z): 1.71 pb (NLO)
- DY: $\text{k}^{NNLO,DY}_{QCD\otimes QED} \approx 1$

- Irreducible jjllnunu: k_NLO = 2
- tWj: 0.51 pb (after cuts, including all relevant branching fractions)

$\sigma_{bknd} \sim 10^5 \sigma_{hh}$

	Signal	$t\bar{t}$	$t\bar{t}h$	$t\bar{t}V$	$\ell\ell bj$	$\tau\tau bb$	$tw+j$	$jj\ell\ell\nu\nu$	σ	S/B
Baseline cuts: $\not{P}_T > 20$ GeV, $p_{T,\ell} > 20$ GeV, $\Delta R_{\ell\ell} < 1.0$, $p_{T,b} > 30$ GeV, $\Delta R_{bb} < 1.3$, $m_{\ell\ell} < 65$ GeV, $95 < m_{bb} < 140$ GeV	0.01046	1.8855	0.0269	0.0179	0.0697	0.0250	0.2209	0.0113	0.38	0.0046

cross section in fb

tt: 84%   tW: 9.8%   DY+jets: 3.1%   tth: 1.2%   tautau + bb: 1.1%   ttV: 0.8%

Dotted lines are baseline cuts.

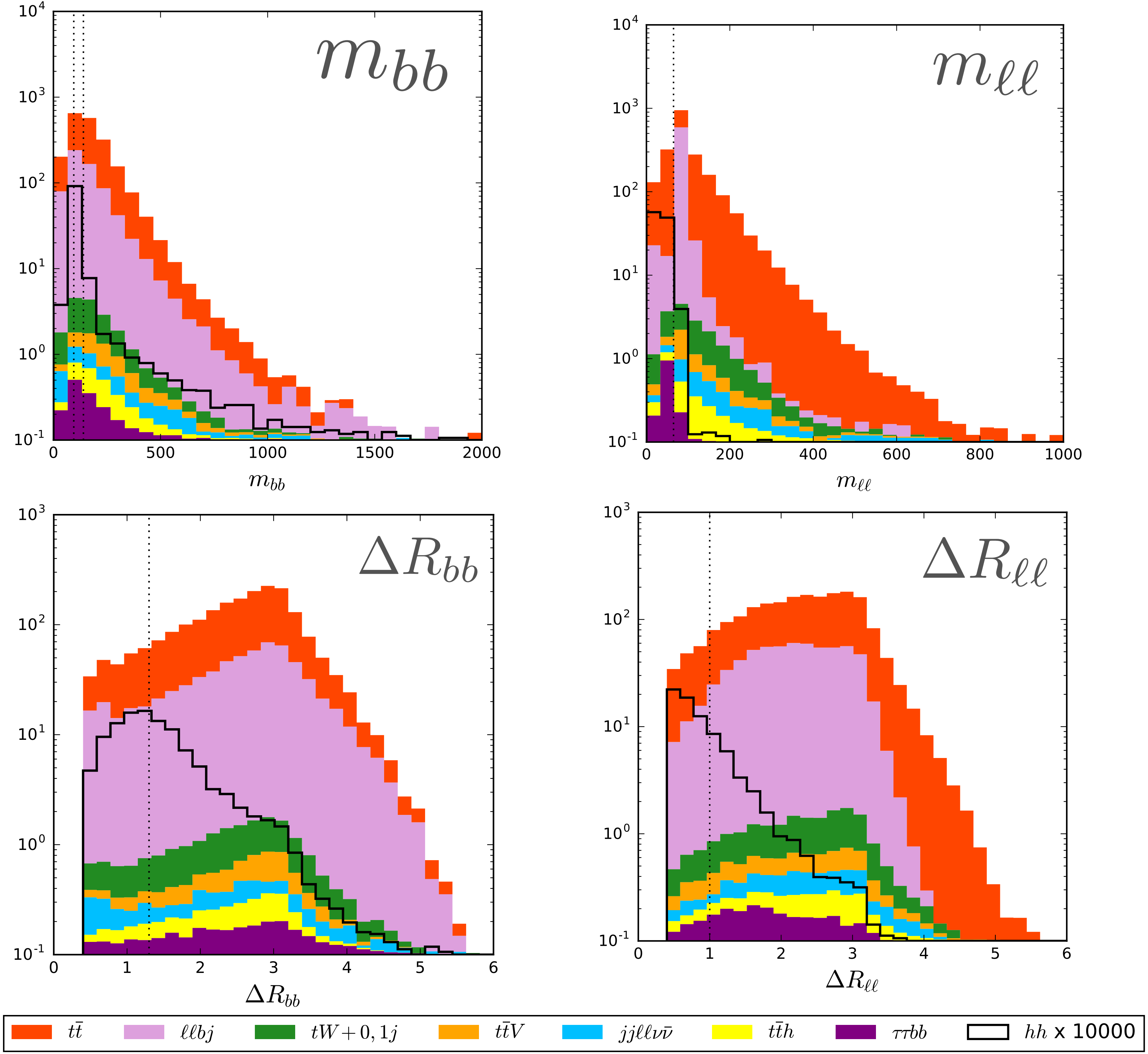

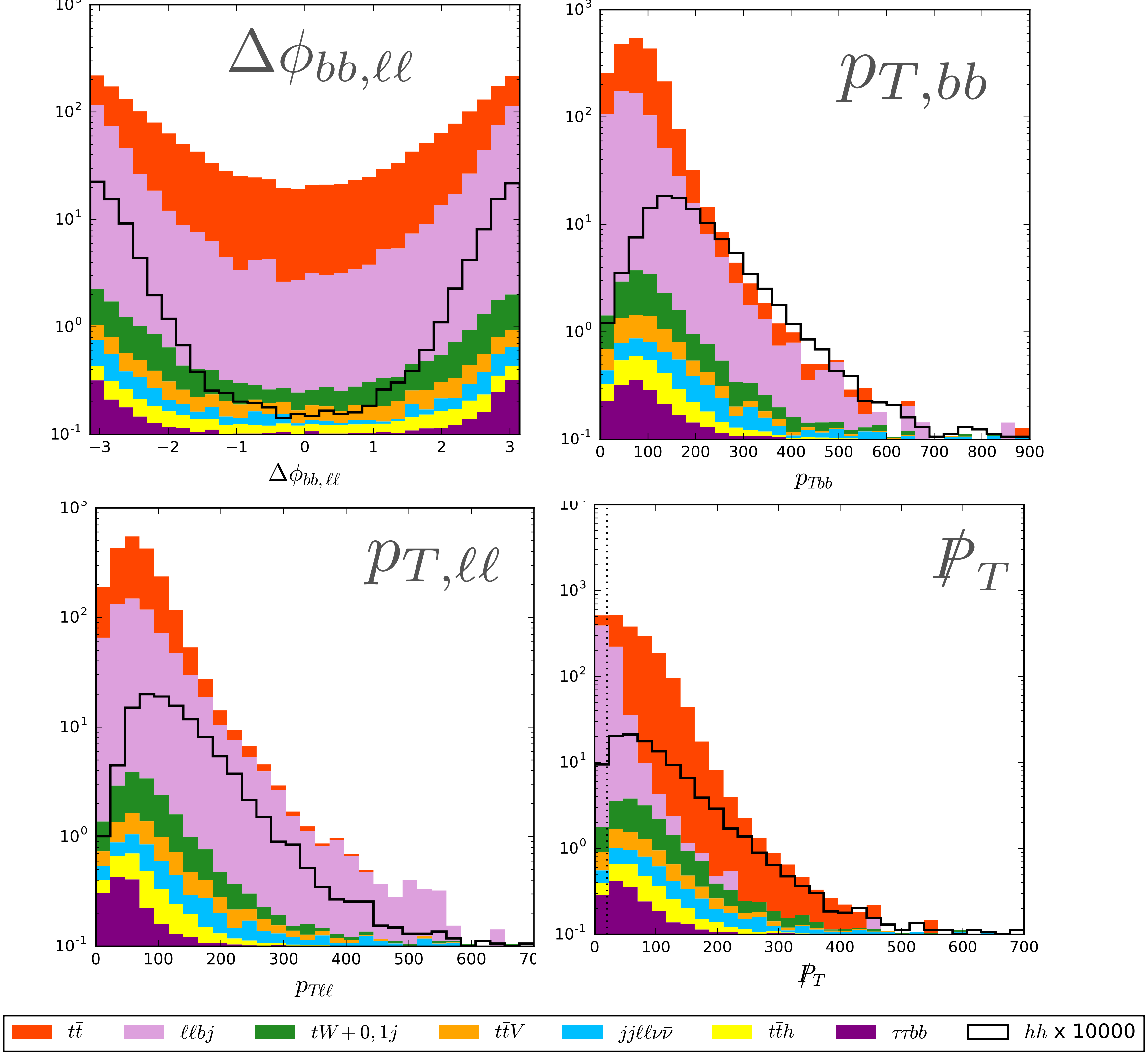

$\Delta\phi_{bb,\ell\ell}$
$p_{T,bb}$
$p_{T,\ell\ell}$
$\not{p}_T$
$\Delta\phi_{bb,\ell\ell}$
p_{Tbb}
$p_{T\ell\ell}$
$\not{p}_T$
$t\bar{t}$
$\ell\ell bj$
$tW+0,1j$
$t\bar{t}V$
$jj\ell\ell\nu\bar{\nu}$
$t\bar{t}h$
$\tau\tau bb$
hh x 10000

How to reduce ttbar background

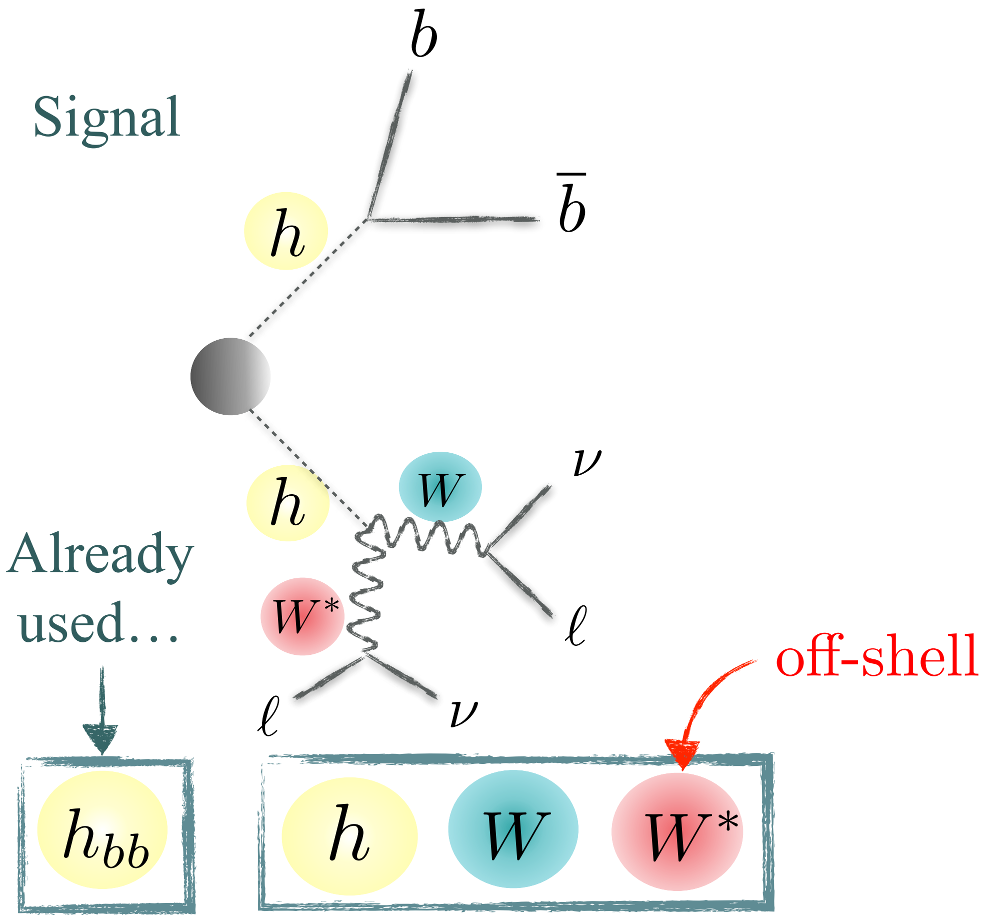

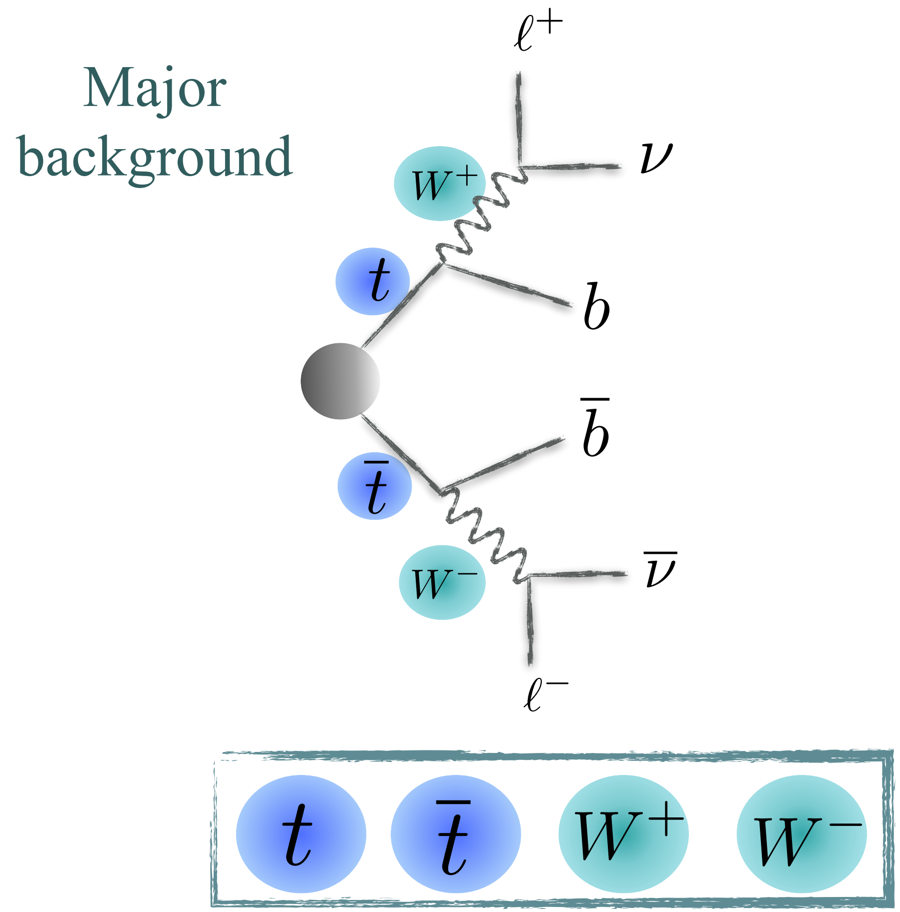

- This can be done with on-shell conditions of particles.
- This information is independent of how these particles are produced.
- Therefore less correlated with other kinematic variables.

Topness (T)

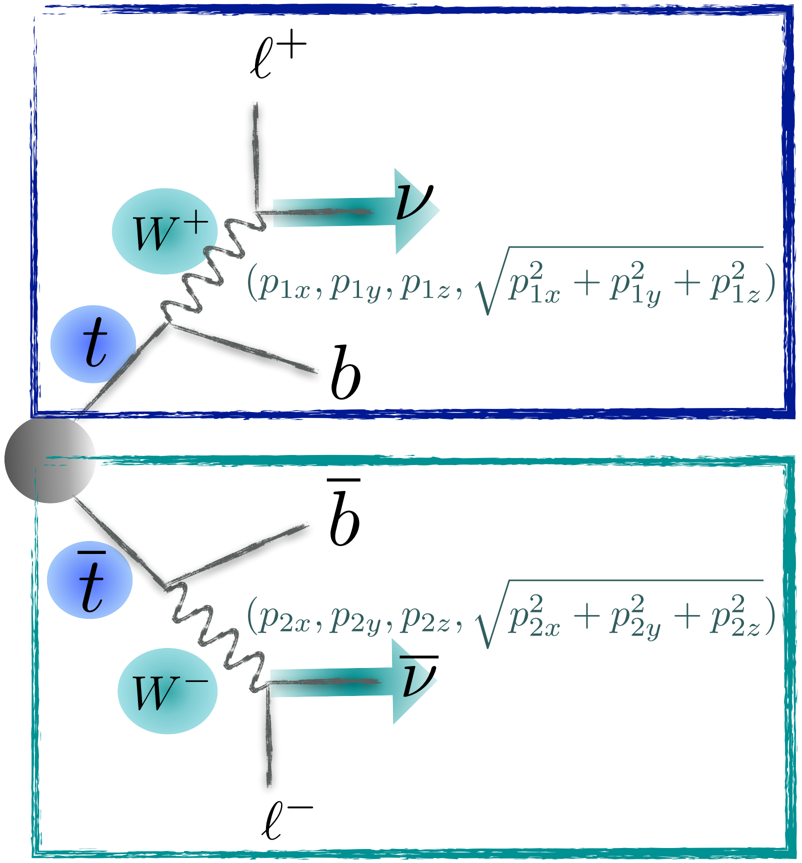

$$\chi^2_{ij} \equiv \min_{\vec{\not{p}}_T = \vec{p}_{\nu T} + \vec{p}_{\bar{\nu} T}} \left[\frac{\left(m^2_{b_i \ell^+ \nu} - m_t^2\right)^2}{\sigma_t^4} + \frac{\left(m^2_{\ell^+ \nu} - m_W^2\right)^2}{\sigma_W^4} + \frac{\left(m^2_{b_j \ell^- \bar{\nu}} - m_t^2\right)^2}{\sigma_t^4} + \frac{\left(m^2_{\ell^- \bar{\nu}} - m_W^2\right)^2}{\sigma_W^4} \right]$$

$$T \equiv min\left(\chi^2_{12}\,,\ \chi^2_{21}\right)$$

two possible ways of paring b and ℓ

- Topness provides a degree of consistency to dileptonic $t\bar{t}$ production.
- It scans over 6 unknowns of neutrino momenta with four on-shell masses and missing E_T constraints.
- And find a minimum of the likelihood function.

Grasser, Shelton, Park, PRL 2013

Kim, Kong, Matchev, Park, PRL 2019

Kim, Kim, Kong, Matchev, Park, JHEP 2019

Higgsness (H)

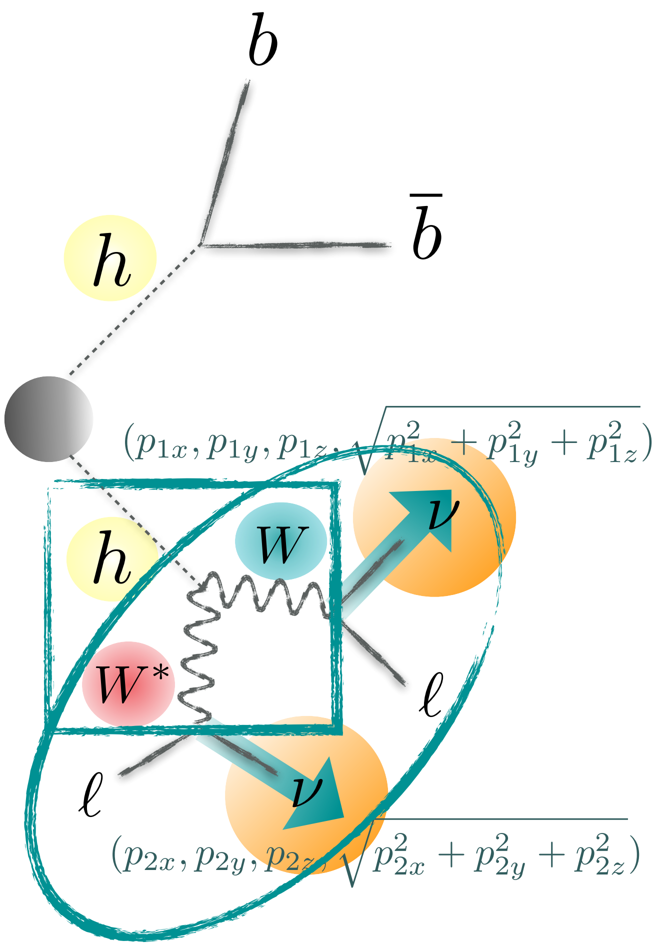

$$H \equiv \min_{\not{\vec{p}}_T = \vec{p}_{\nu T} + \vec{p}_{\bar{\nu} T}} \left[\frac{\left(m^2_{\ell^+\ell^-\nu\bar{\nu}} - m_h^2\right)^2}{\sigma^4_{h_\ell}} + \frac{\left(m^2_{\nu\bar{\nu}} - m^2_{\nu\bar{\nu},peak}\right)^2}{\sigma^4_{\nu}} + min\left(\frac{\left(m^2_{\ell^+\nu} - m_W^2\right)^2}{\sigma^4_W} + \frac{\left(m^2_{\ell^-\bar{\nu}} - m^2_{W^*,peak}\right)^2}{\sigma^4_{W_*}}, \frac{\left(m^2_{\ell^-\bar{\nu}} - m_W^2\right)^2}{\sigma^4_W} + \frac{\left(m^2_{\ell^+\nu} - m^2_{W^*,peak}\right)^2}{\sigma^4_{W_*}} \right) \right],$$

two possible ways of paring ν and ℓ

$\sim m_h - m_W$ off-shell

- Higgsness provides a degree of consistency to dileptonic $h \to WW^*$ system.
- The off-shell W also has an end-point near m_h - m_W.
- Its distribution is wide, but there is a peak, which can constrain hh system further.

Kim, Kong, Matchev, Park, PRL 2019

Kim, Kim, Kong, Matchev, Park, JHEP 2019

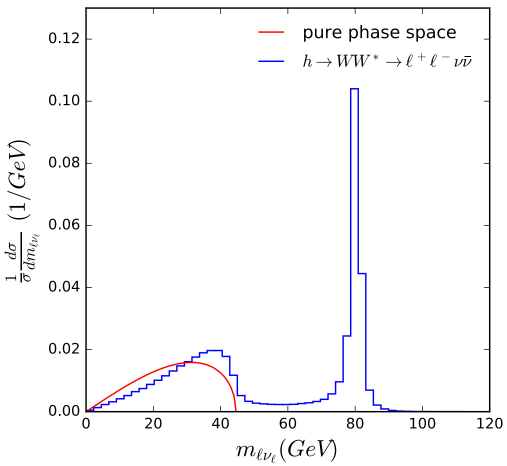

$$m_{W^*}^{peak} = \frac{1}{\sqrt{3}}\sqrt{2\left(m_h^2 + m_W^2\right) - \sqrt{m_h^4 + 14m_h^2m_W^2 + m_W^4}}$$

$$E = \sqrt{m_W m_{W^*}\, e^{\eta}}\,,$$

$$\cosh\eta = \left(\frac{m_h^2 - m_W^2 - m_{W^*}^2}{2m_W m_{W^*}}\right)$$

$$\ldots + \frac{\left(m_{\nu\bar{\nu}}^2 - m_{\nu\bar{\nu},peak}^2\right)^2}{\sigma_\nu^4}$$

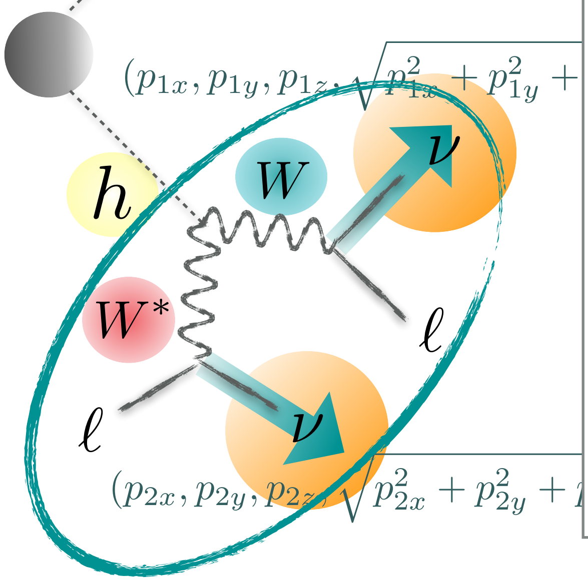

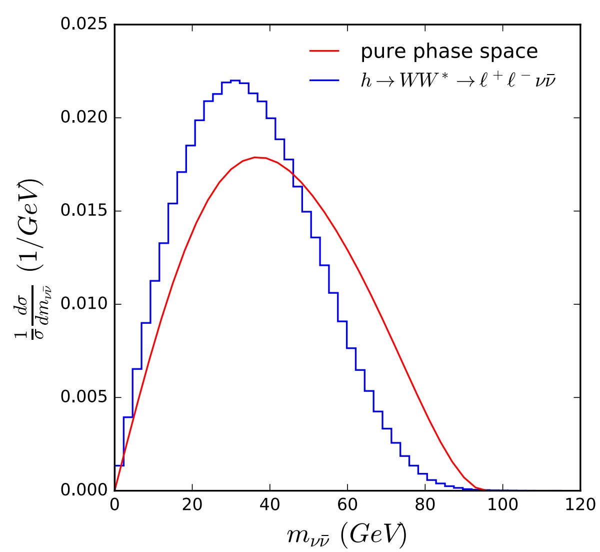

$$\frac{d\sigma}{dm_{\nu\bar{\nu}}} \propto \int dm_{W^*}^2 \lambda^{1/2}(m_h^2, m_W^2, m_{W^*}^2) f(m_{\nu\bar{\nu}})$$

$$f(m) \sim \begin{cases} \eta\, m\,, & 0 \le m \le e^{-\eta}E, \\ m\ln(E/m)\,, & e^{-\eta}E \le m \le E, \end{cases}$$

$$\lambda(x,y,z) = x^2 + y^2 + z^2 - 2xy - 2yz - 2zx$$

off-shell

- Higgsness provides a degree of consistency to dileptonic $h \to WW^*$ system.
- The off-shell W also has an end-point near m_h - m_W.
- Its distribution is wide, but there is a peak, which can constrain hh system further.

Kim, Kong, Matchev, Park, PRL 2019
Kim, Kim, Kong, Matchev, Park, JHEP 2019

Distributions of (*log H* , *log T*) after baseline selection cuts

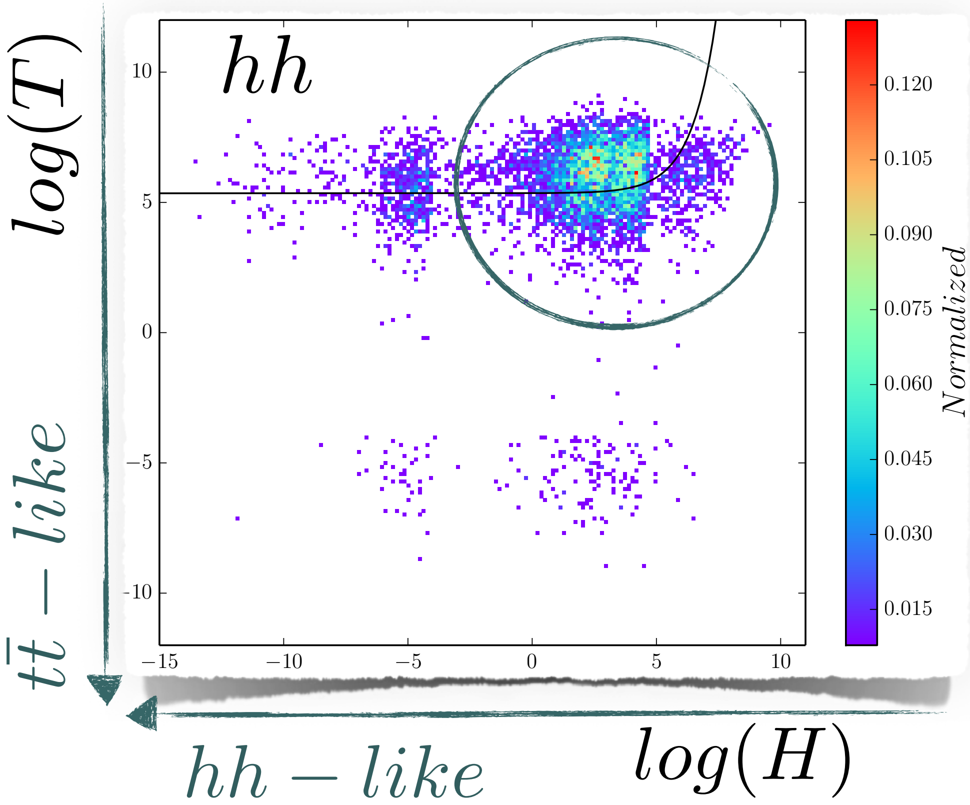

- A clear separation between *hh* and backgrounds ($t\bar{t}$ is dominant)

All backgrounds

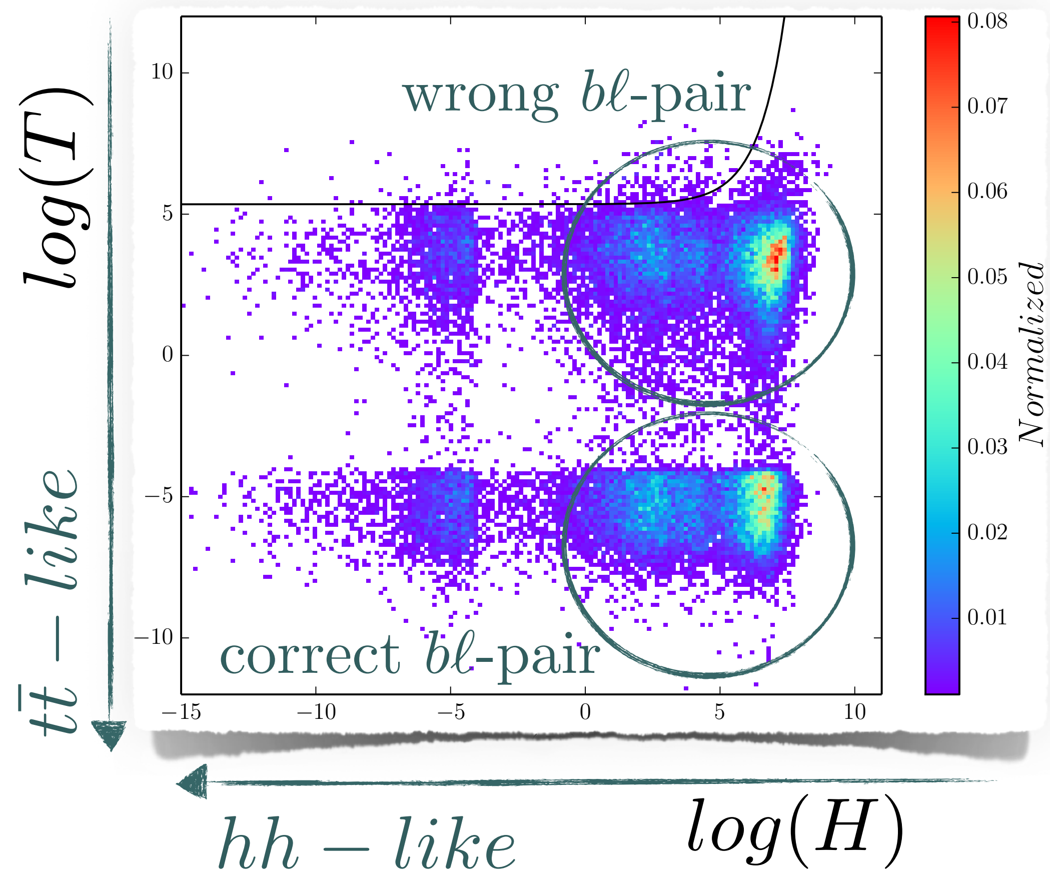

- Since there is a two-fold ambiguity in $b\ell$-paring, Topness displays the island-nature.

How to rescue $bbWW^*$?

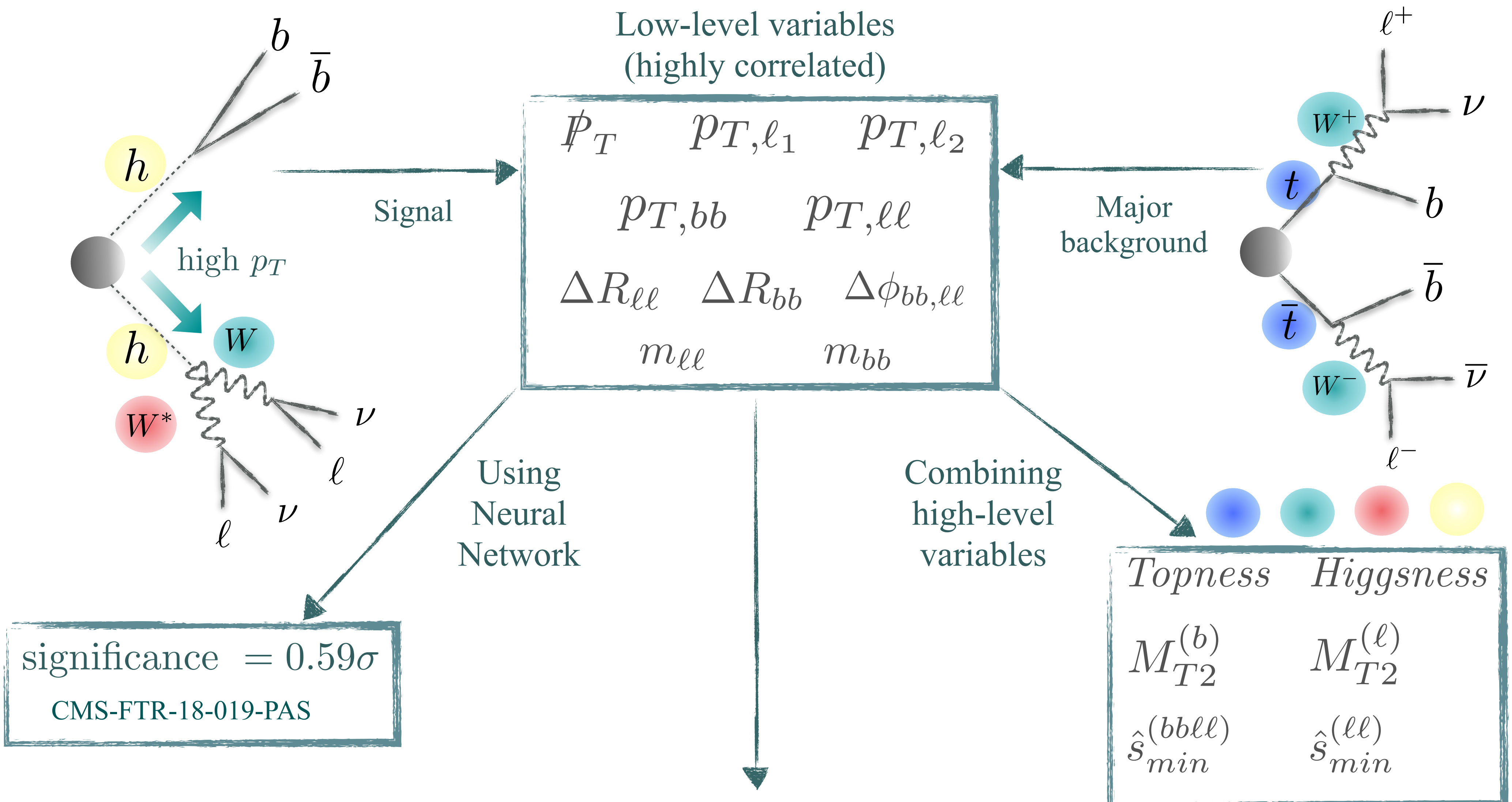

We utilize jet images, and let the machine deal with correlations.

Kim, Kong, Matchev, Park, PRL 2019
Kim, Kim, Kong, Matchev, Park, JHEP 2019

Processing Hadron Images (hh)

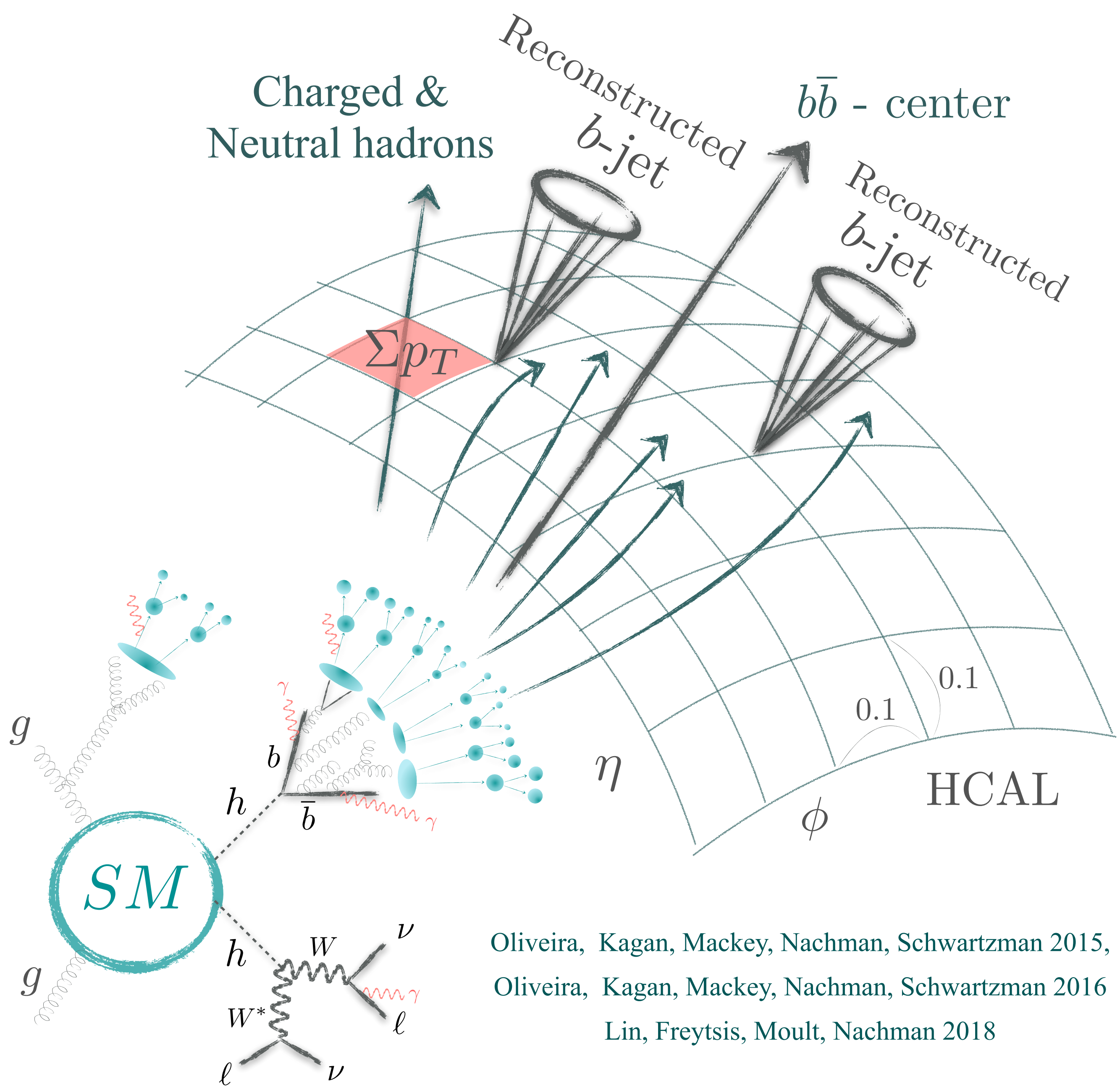

Oliveira, Kagan, Mackey, Nachman, Schwartzman 2015,
Oliveira, Kagan, Mackey, Nachman, Schwartzman 2016
Lin, Freytsis, Moult, Nachman 2018

Each event

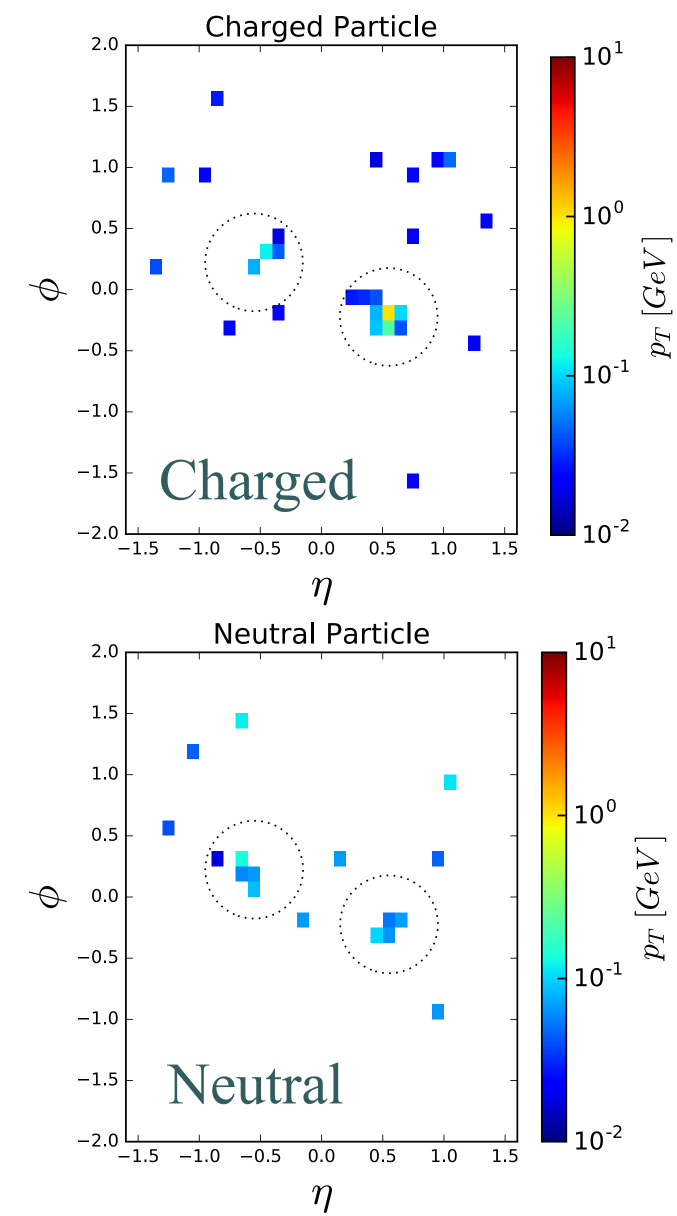

Kim, Kong, Matchev, Park JHEP 2019

Processing Hadron Images (hh)

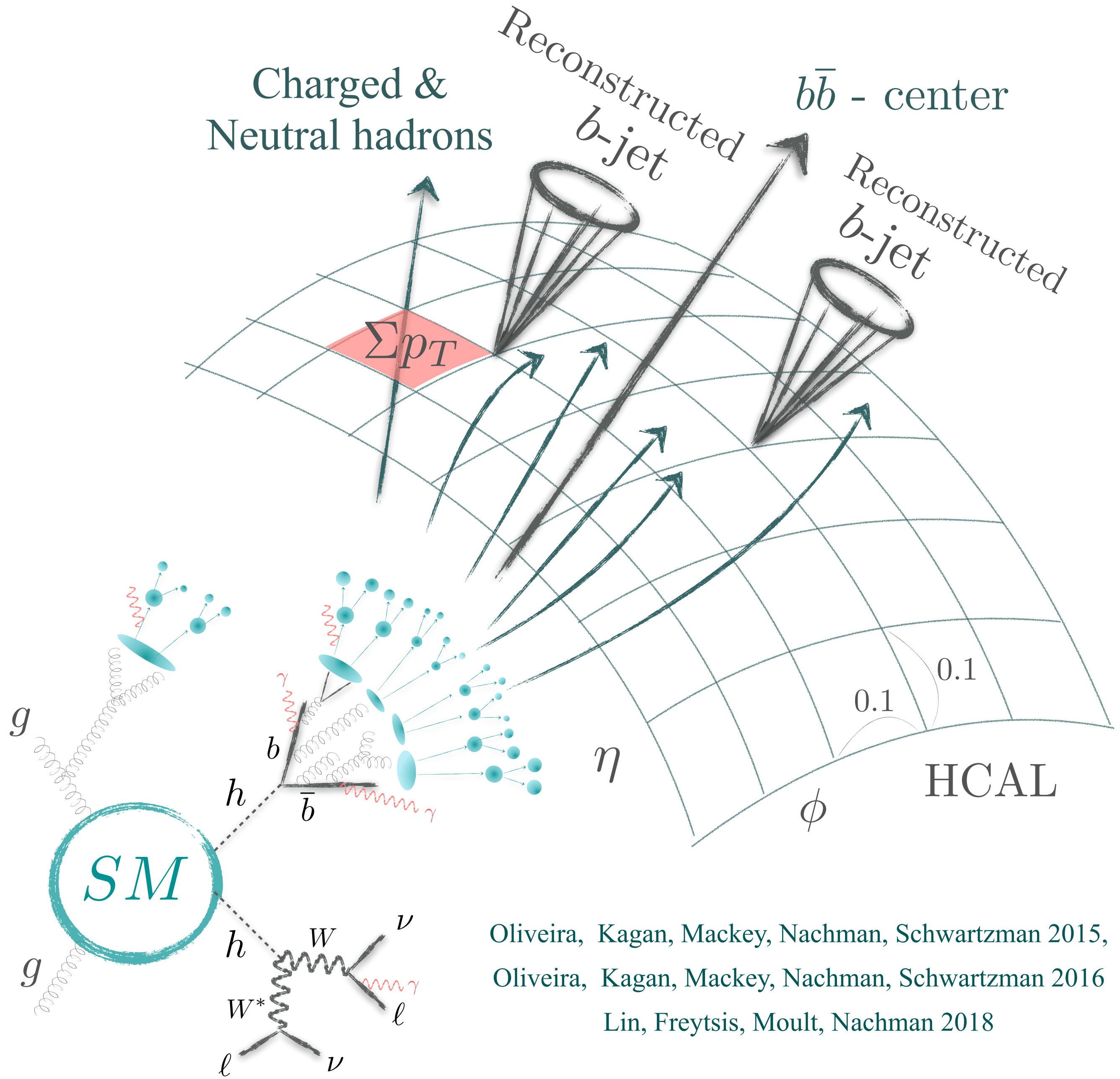

Sum of all events

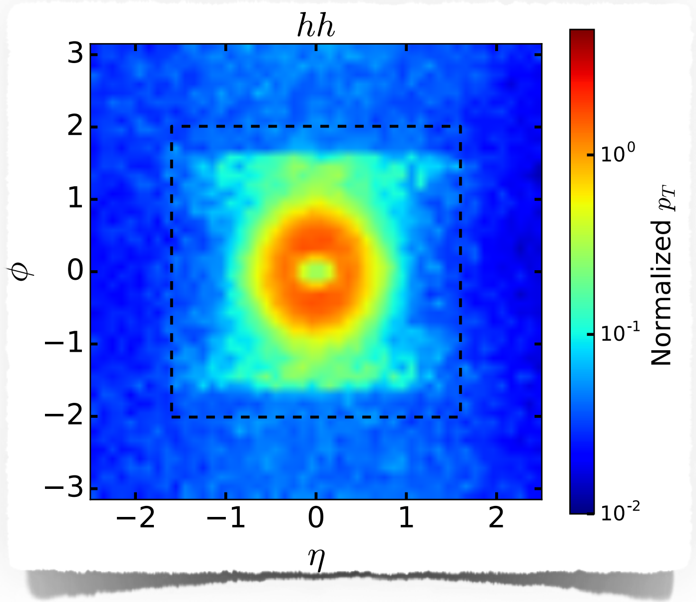

Oliveira, Kagan, Mackey, Nachman, Schwartzman 2015,

Oliveira, Kagan, Mackey, Nachman, Schwartzman 2016

Lin, Freytsis, Moult, Nachman 2018

Kim, Kong, Matchev, Park JHEP 2019

Processing Hadron Images (tt)

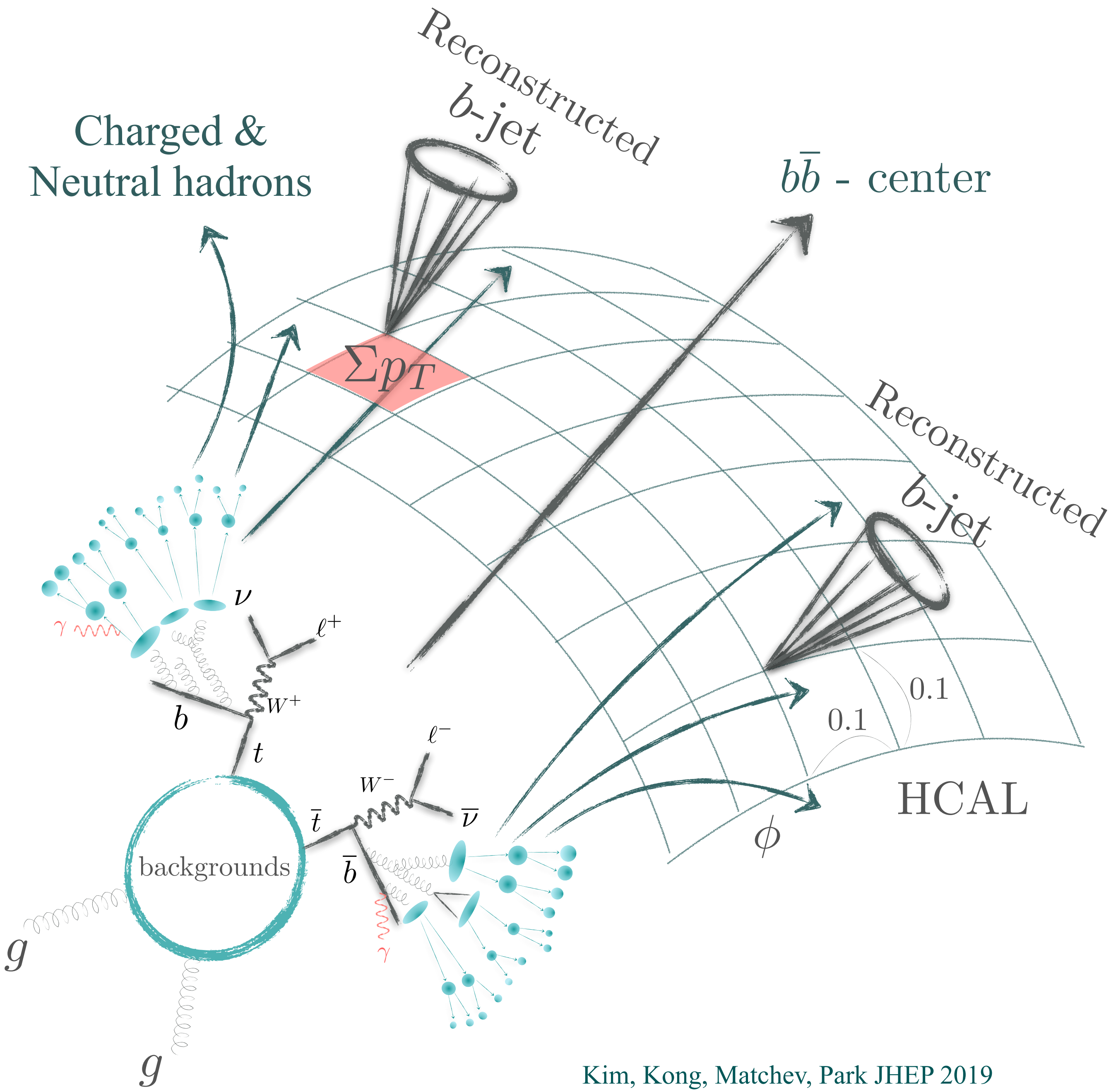

Each event

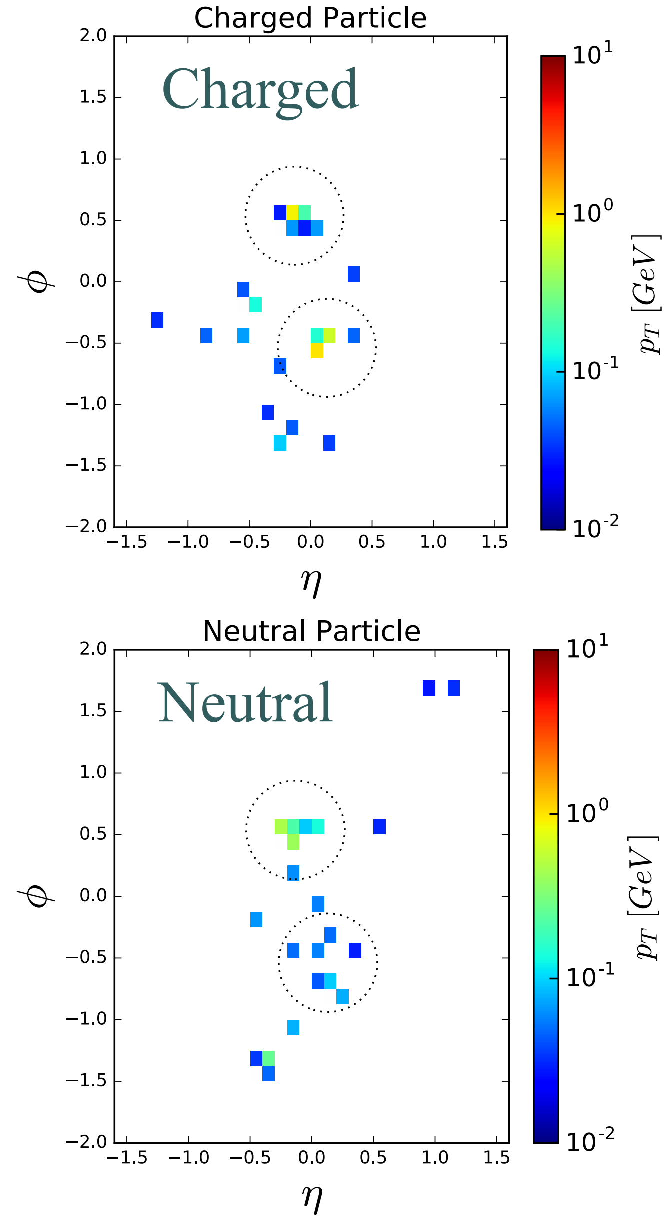

Kim, Kong, Matchev, Park JHEP 2019

Processing Hadron Images (tt)

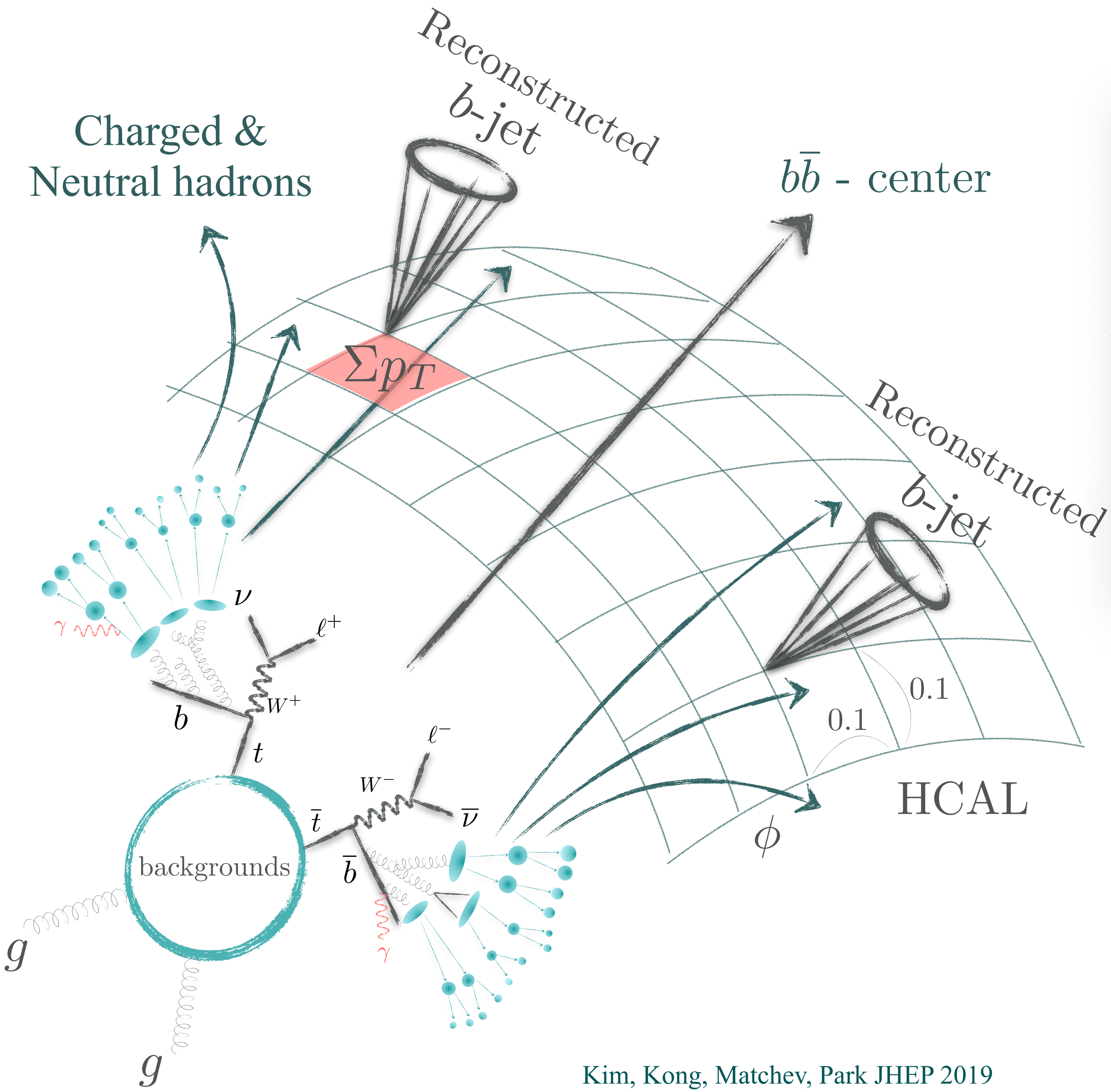

Sum of all events

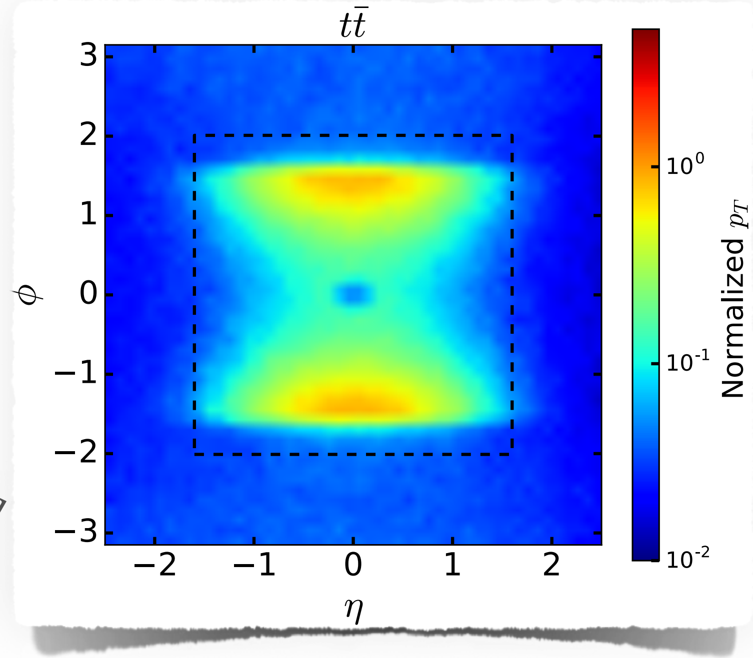

Kim, Kong, Matchev, Park JHEP 2019

Jet images before baseline cuts

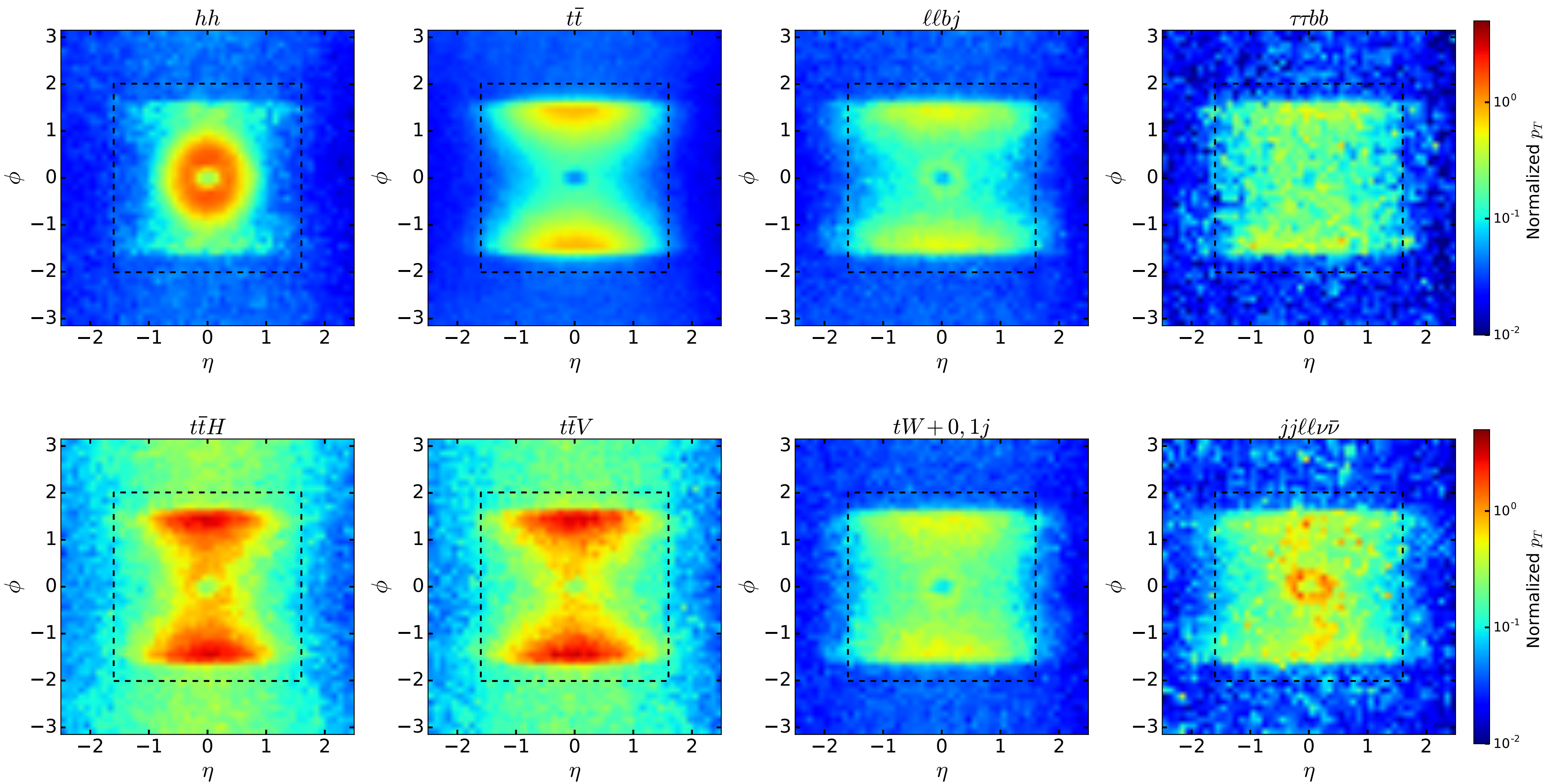

Jet images after baseline cuts

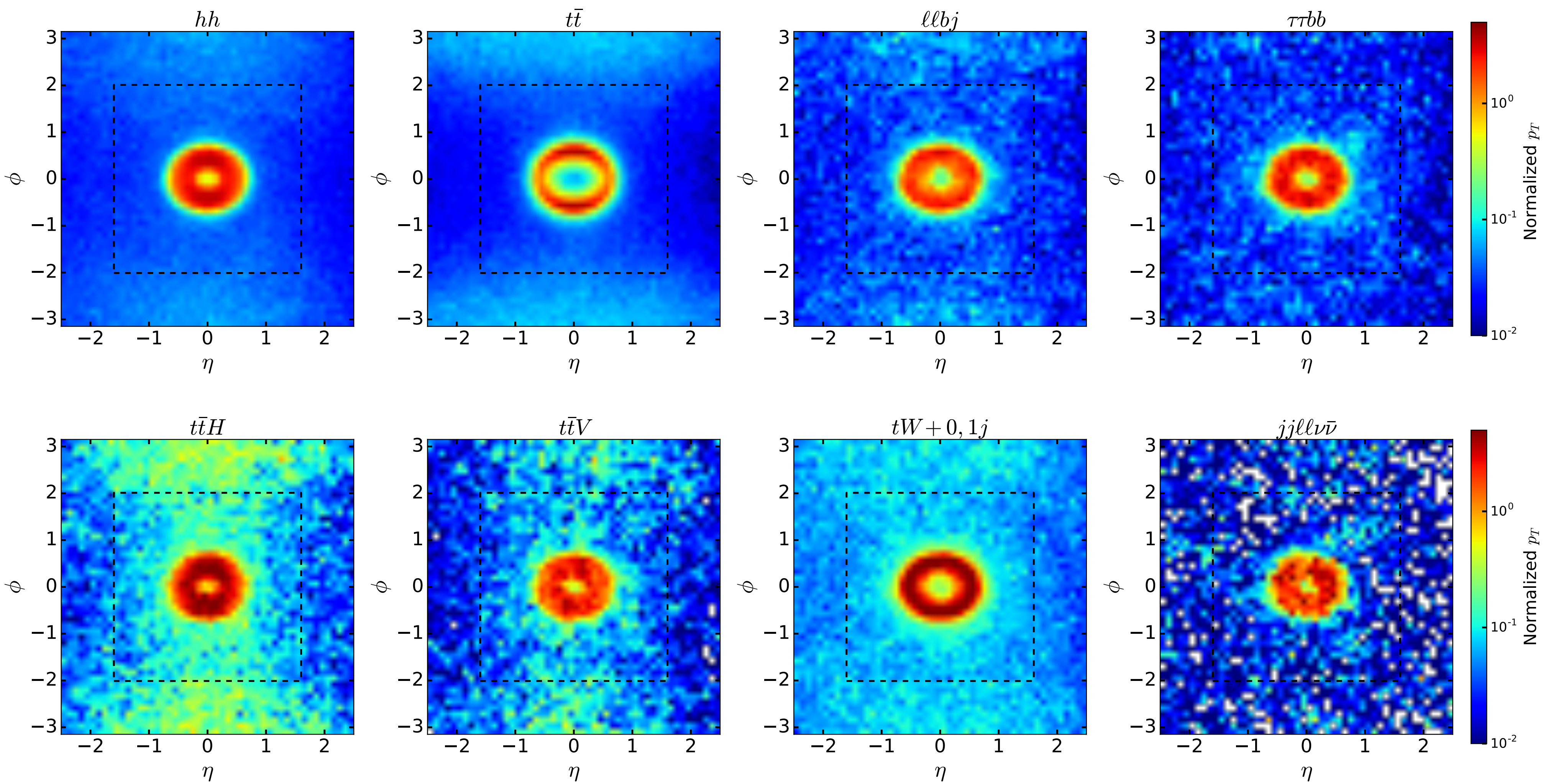

Combining dense neural networks

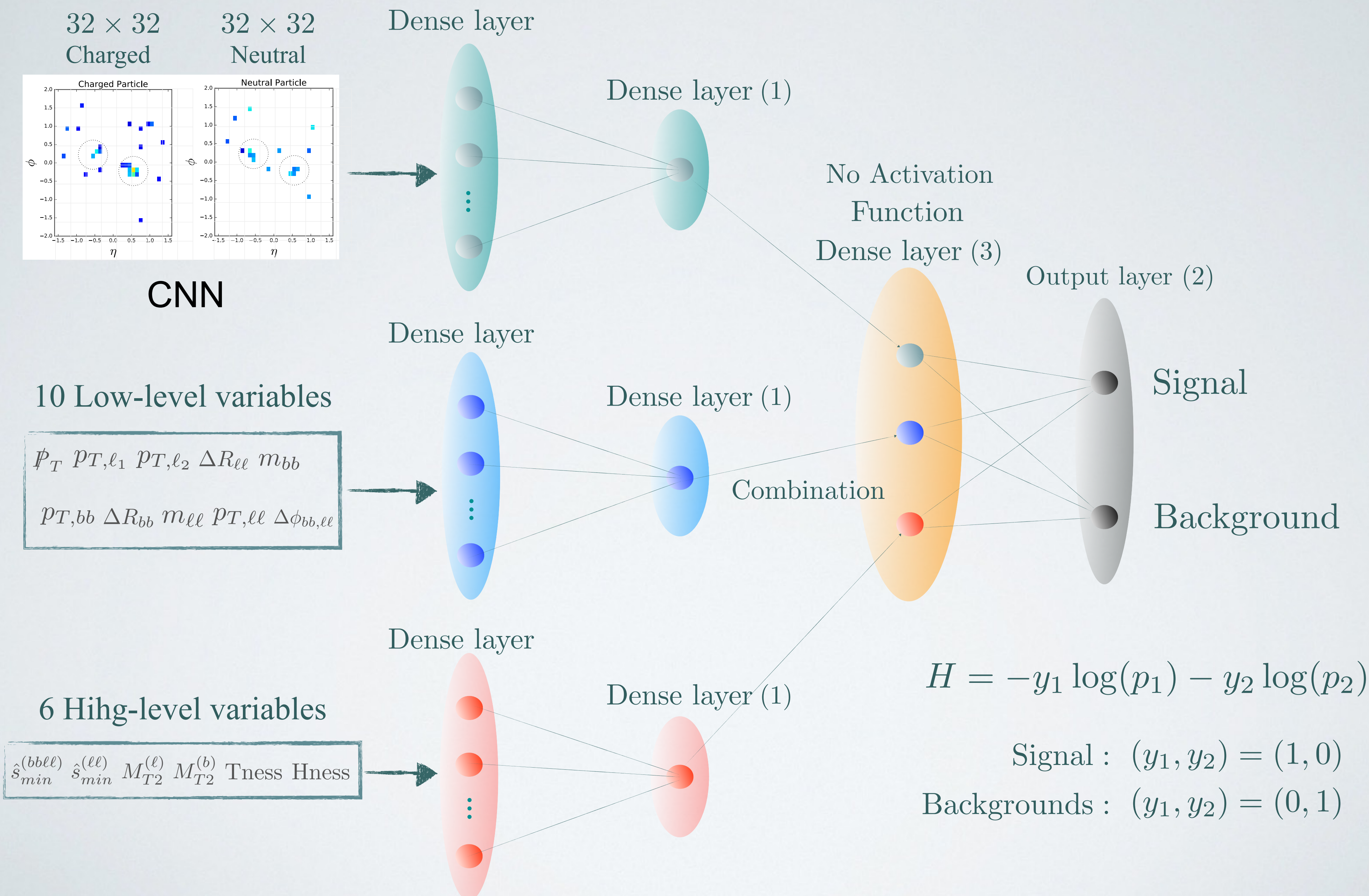

DNN results

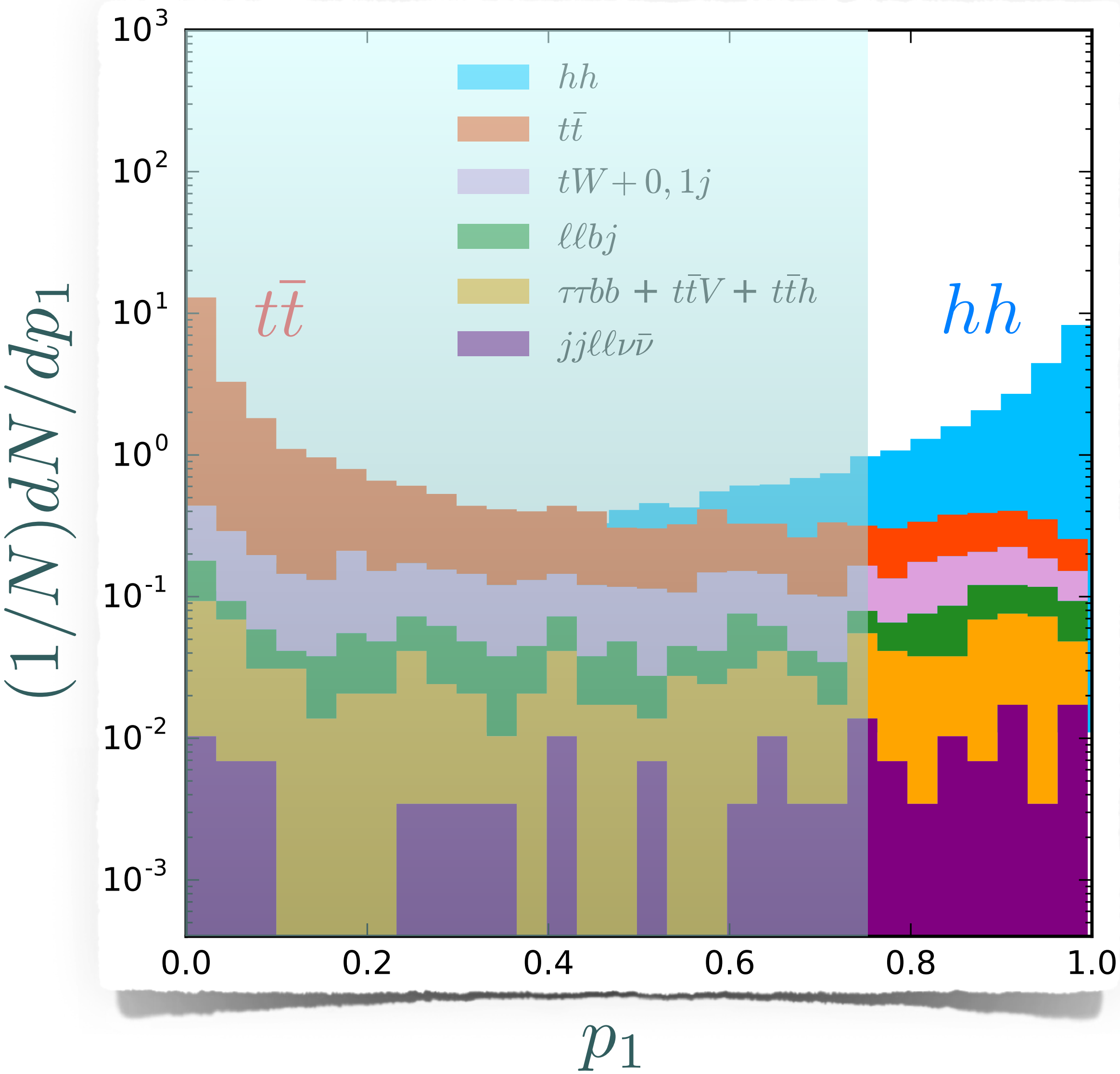

- Once the training is complete, we compute the probability (p_1) that a given event is classified as *hh*.
- Most of backgrounds are unlikely to be classified as *hh*.
- We place a cut on p_1 to disentangle the backgrounds.

$hh \to bbWW^*$ discovery sigfinicance

Using Delphes

$3\ \mathrm{ab}^{-1}(14\ \mathrm{TeV})$

$c_3 = 1$

$\text{significance} \ = 0.59\sigma$

CMS-FTR-18-019-PAS

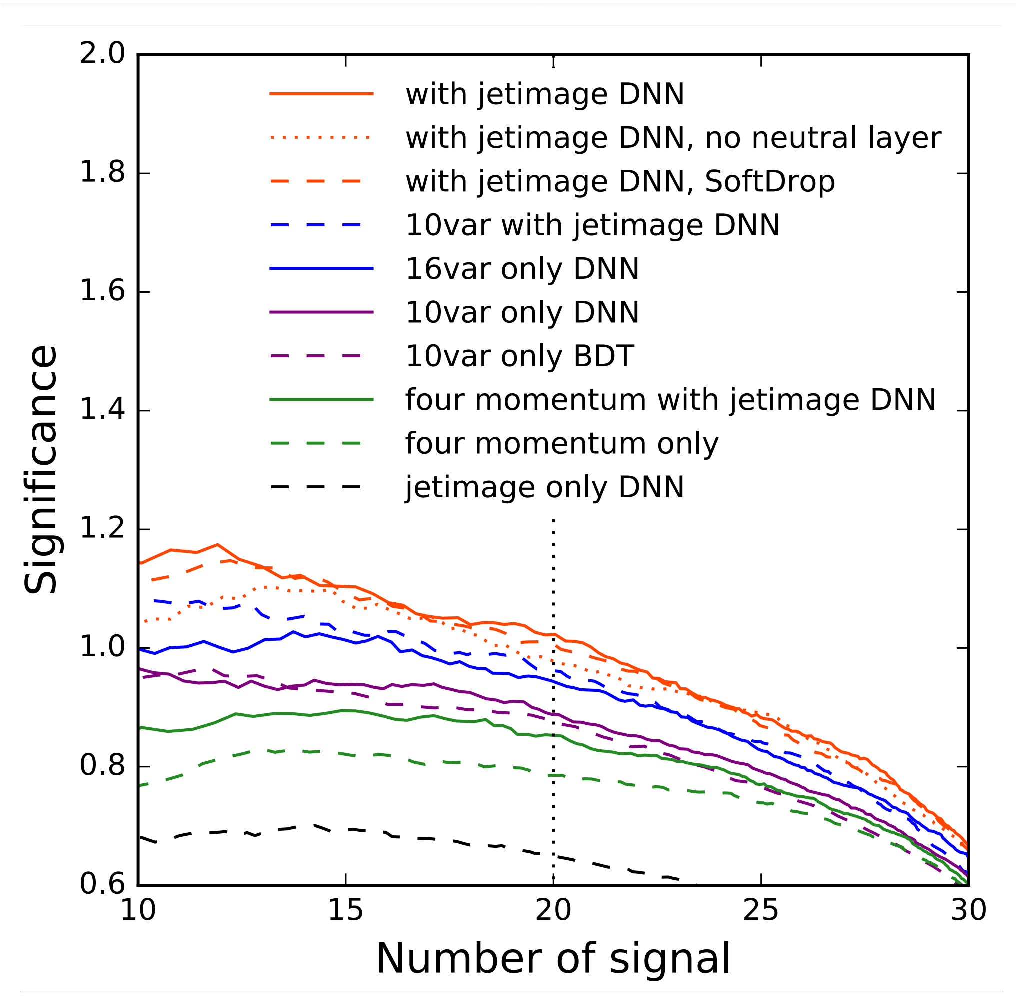

- We can see a relative improvement in each layer of information.
- The DNN with jet images and high-level variables improves the final significance.

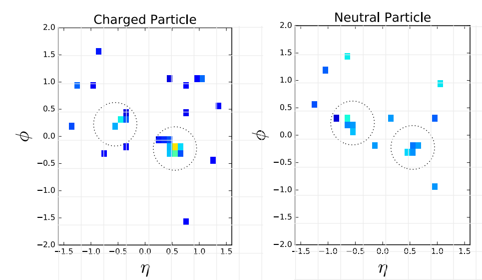

$+$

6 Hihg-level variables

$\hat{s}^{(bb\ell\ell)}_{min}\ \hat{s}^{(\ell\ell)}_{min}\ M^{(\ell)}_{T2}\ M^{(b)}_{T2}$ Tness Hness

$+$

10 Low-level variables

$\not{p}_T\ p_{T,\ell_1}\ p_{T,\ell_2}\ \Delta R_{\ell\ell}\ m_{bb}$

$p_{T,bb}\ \Delta R_{bb}\ m_{\ell\ell}\ p_{T,\ell\ell}\ \Delta\phi_{bb,\ell\ell}$

	Signal	$t\bar{t}$	$t\bar{t}h$	$t\bar{t}V$	$\ell\ell bj$	$\tau\tau bb$	$tw+j$	$jj\ell\ell\nu\nu$	σ	S/B
Baseline cuts: $\not{p}_T > 20$ GeV, $p_{T,\ell} > 20$ GeV, $\Delta R_{\ell\ell} < 1.0$, $p_{T,b} > 30$ GeV, $\Delta R_{bb} < 1.3$, $m_{\ell\ell} < 65$ GeV, $95 < m_{bb} < 140$ GeV	0.01046 63%	1.8855 3%	0.0269 29%	0.0179 17%	0.0697 25%	0.0250 32%	0.2209 14%	0.0113 36%	0.38	0.0046
jet-image DL	0.00667	0.1817	0.0133	0.00793	0.0245	0.0129	0.0671	0.00854	0.65	0.021
10 low-level variables DL	0.00668	0.0806	0.00897	0.00435	0.0163	0.00876	0.0462	0.00578	0.88	0.039
16 variables DL	0.00667	0.0662	0.00948	0.00358	0.0170	0.00747	0.0387	0.00402	0.95	0.046
10 variables + jet-image DL	0.00667	0.0693	0.00897	0.00435	0.0178	0.00722	0.0359	0.00352	0.95	0.045
16 variables + jet-image DL	0.00668	0.0607	0.00769	0.00281	0.0173	0.00799	0.0317	0.00402	1.0	0.051

Table 1. Signal and background cross sections in fb after baseline cuts (first row) and at different stages of analysis, using a combination of kinematic variables and jet images while requiring $N = 20$ signal events. The significance σ is calculated using the log-likelihood ratio for a luminosity of 3 ab^{-1} at the 14 TeV LHC.

tt: 84% tautau + bb: 1.1%
tW: 9.8% tth: 1.2%
DY+jets: 3.1% ttV: 0.8%

→

tt: 46% tautau + bb: 6%
tW: 24% tth: 5.8%
DY+jets: 13% ttV: 2.1%

The Di-Higgs Photography

- Totally hadrons, lepton, photon, and neutrino images are shown for hh.

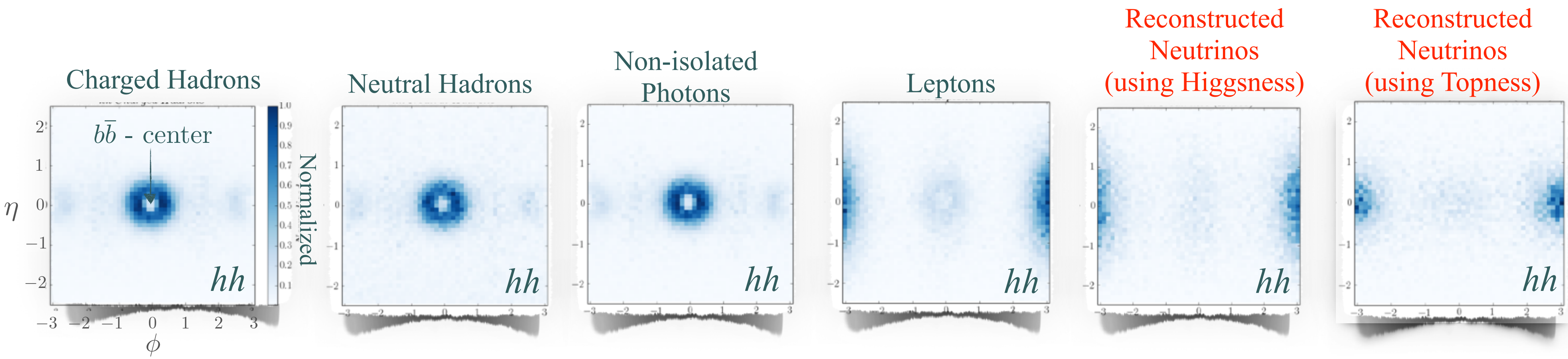

- Analogous images are shown for $t\bar{t}$ background.

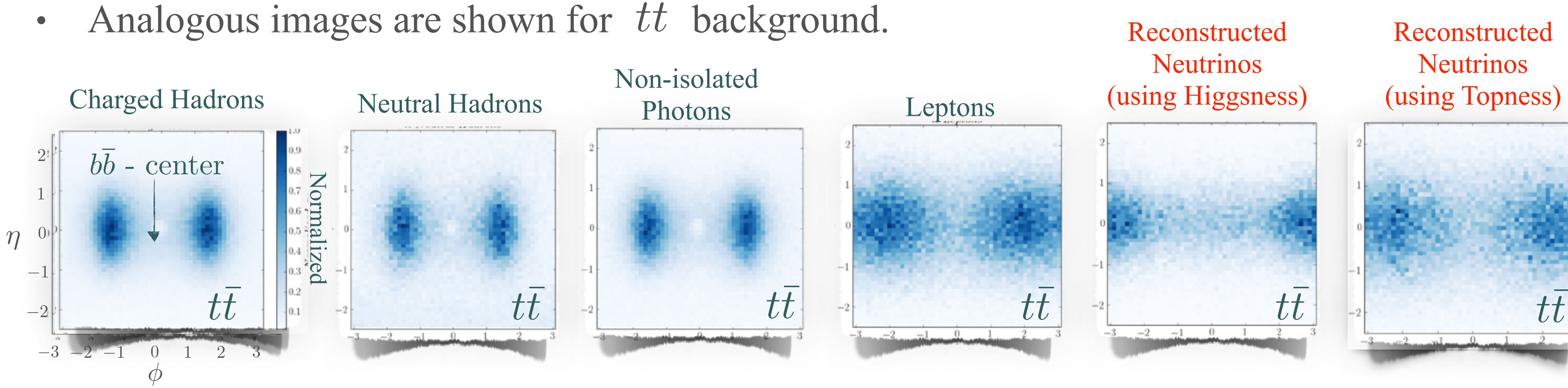

- A sharp difference between hh and $t\bar{t}$.
- Construct 5 images (L+T, L+H) with 6 images data set.

Kim, Kim, Kong, Matchev, Park, preliminary

Combining image data and high level kinematic variables in dense neural networks

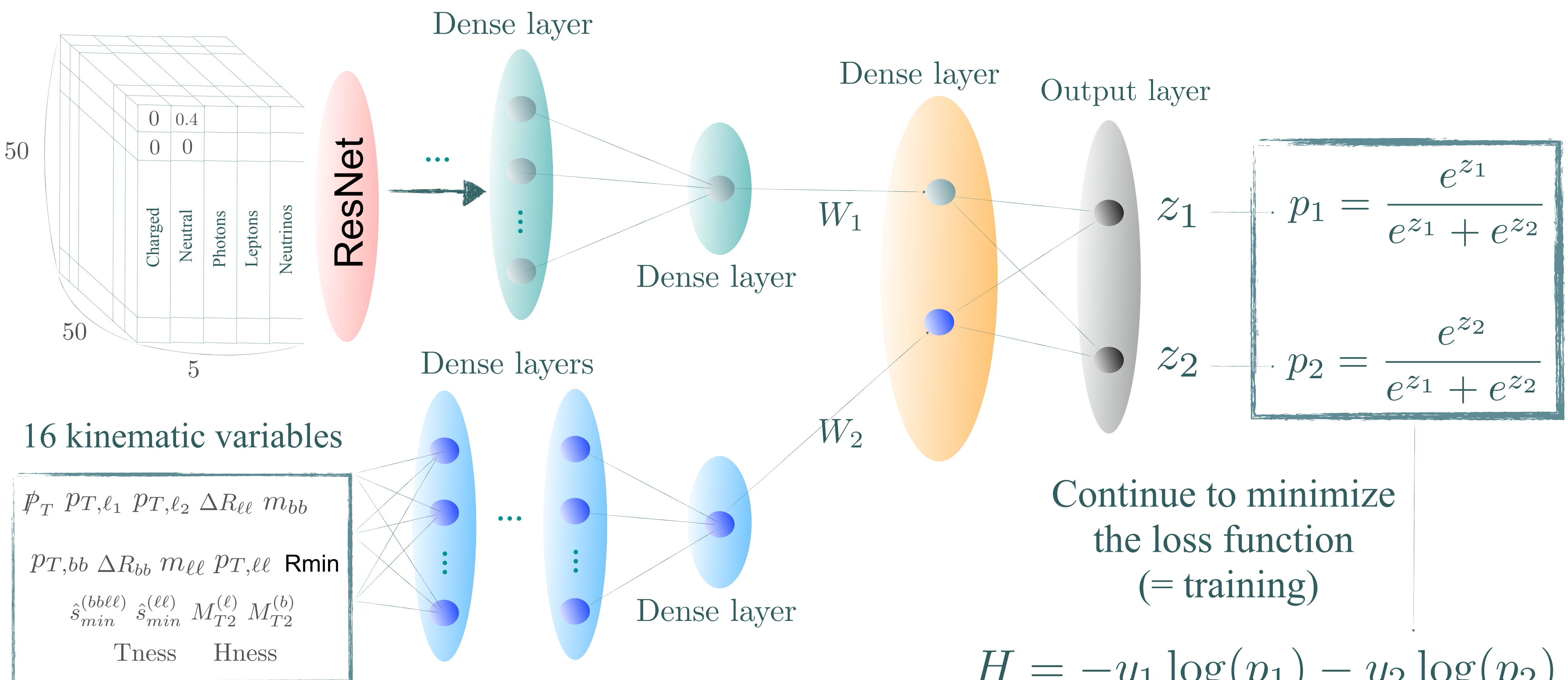

Continue to minimize the loss function (= training)

$$H = -y_1 \log(p_1) - y_2 \log(p_2)$$

$$\text{Signal}: \quad (y_1, y_2) = (1, 0)$$

$$\text{Backgrounds}: \quad (y_1, y_2) = (0, 1)$$

Kim, Kim, Kong, Matchev, Park, preliminary

Preliminary Results

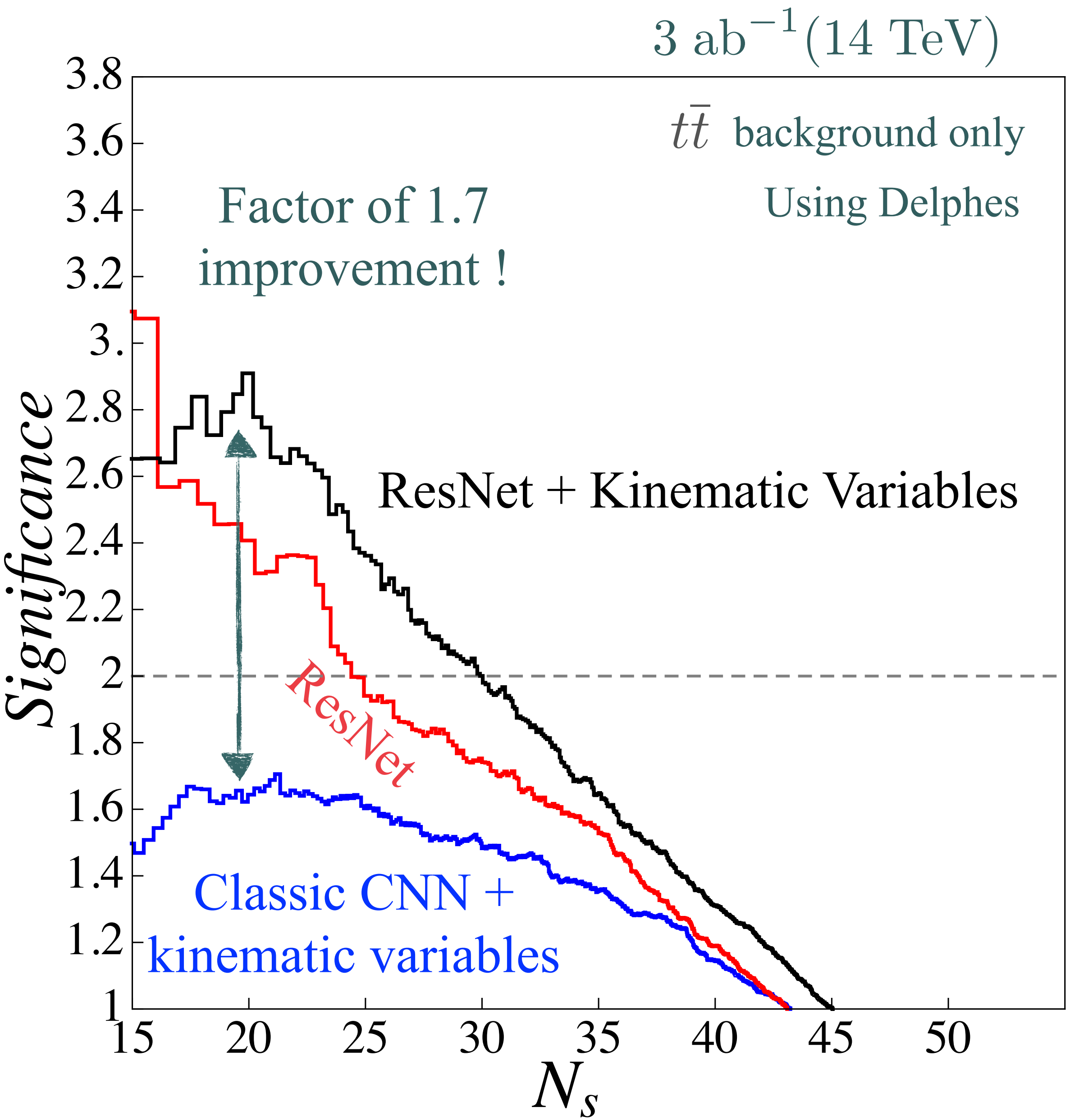

- As a preliminary study, we included only $t\bar{t}$ background.
- Significance with kinematic variables only or jet images only give signal significance below 1.
- We find that the classic CNN + kinematic variables can reach at most 1.6 sigma.
- Our ResNet can be further reinforced by combining reconstructed kinematic variables.
- More recent architecture, Capsule Nets also provides a similar performance.

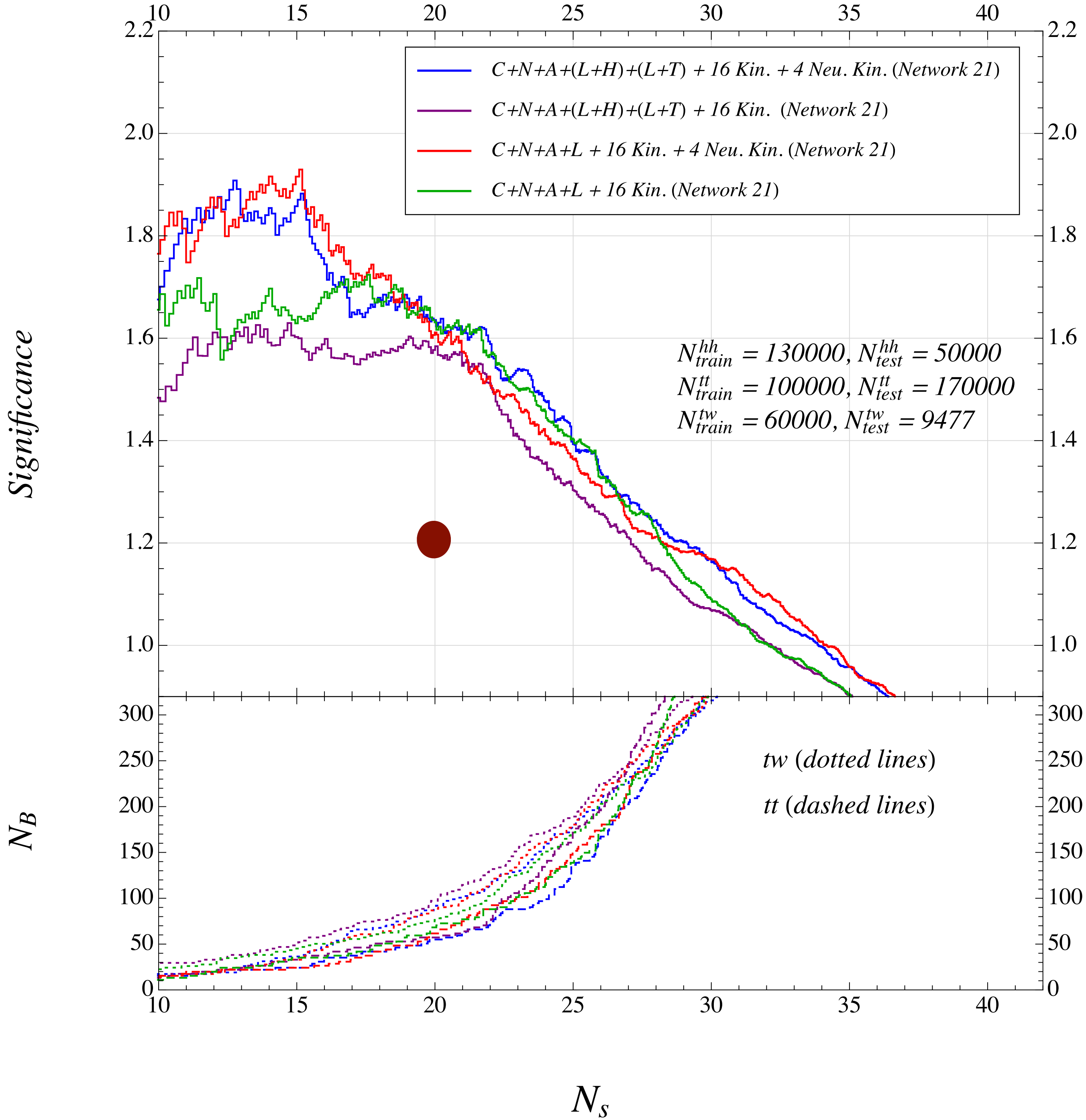

- With tt + tW backgrounds, CNN+kinematic variables leads to significance of ~1.2
- ResNets brings ~30% improvement with additional features such as lepton and neutrino images.

Neutrino momenta (parton-level)

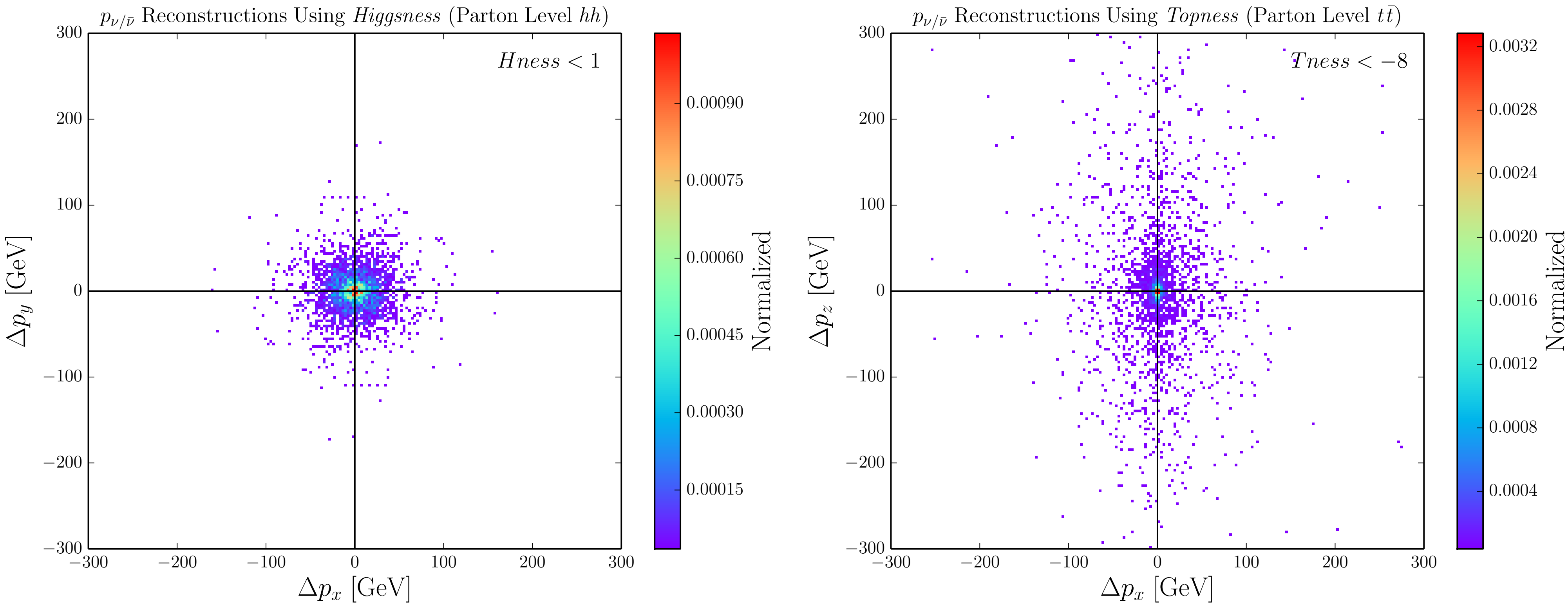

- Just like MT2, Higgsness and Topness provide momentum of neutrinos.
- They can be used to study other quantities.

Shape variables (Parton Level)

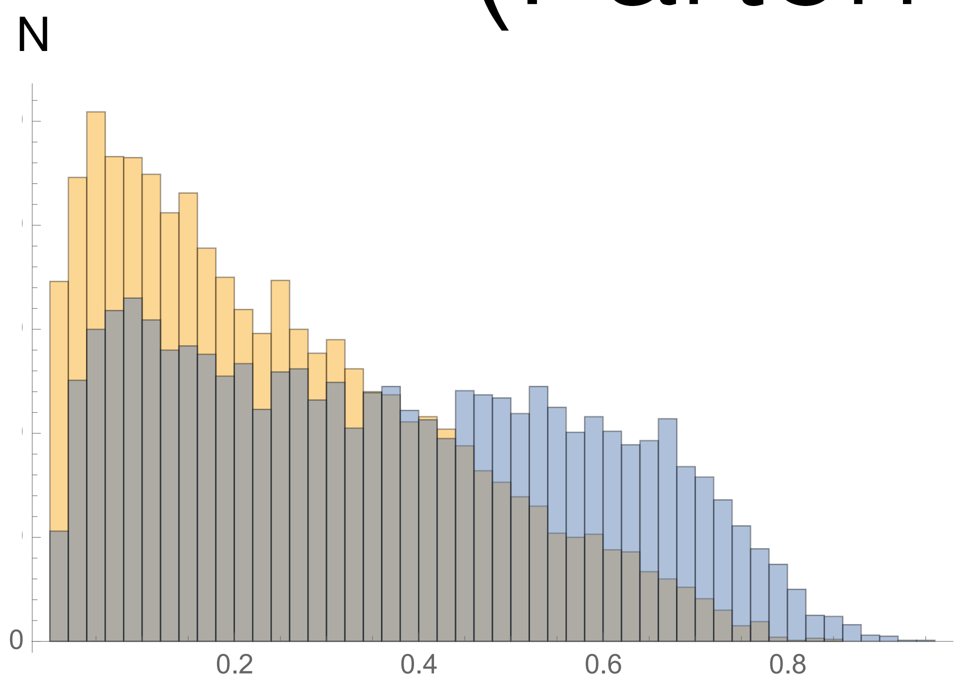

Sphericity in lab frame

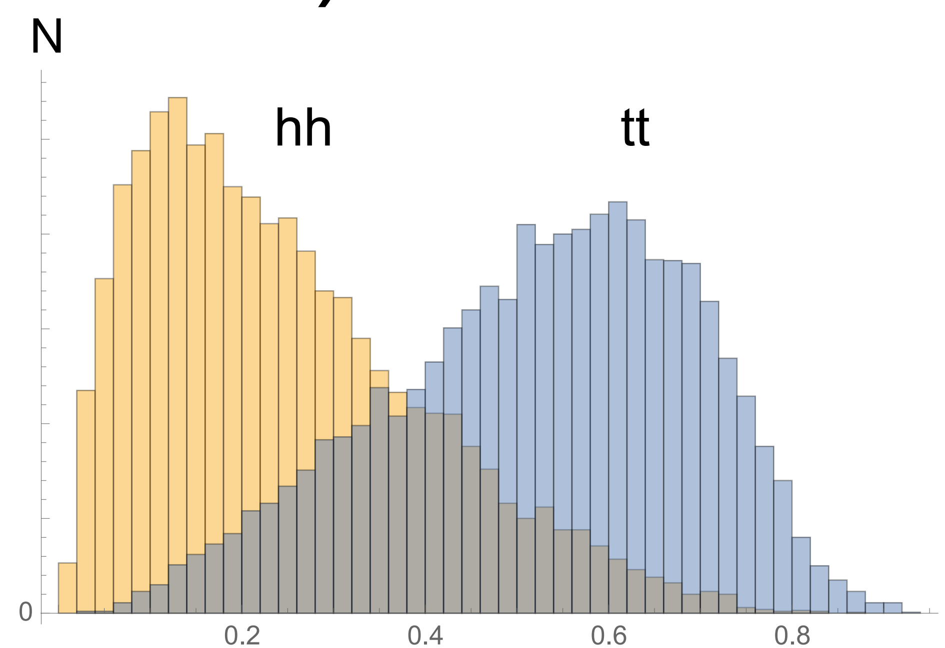

Sphericity in CM frame

$$S^{\alpha\beta} = \frac{\sum_i p_i^\alpha p_i^\beta}{\sum_i \mid p_i \mid^2}, \quad \lambda_1 + \lambda_2 + \lambda_3 = 1$$

$$\lambda_1 \geq \lambda_2 \geq \lambda_3$$

$$S = \frac{3}{2}(\lambda_2 + \lambda_3)$$

- S -> 0: pencil-like event
- S -> 1: isotropic event

Chen, Kozaczuk, Lewis, 1704.05844, Non-resonant Collider Signatures of a Singlet-Driven Electroweak Phase Transition

Alhazmi, Kim, Kong, Lewis, preliminary

Exclusion (yellow) and discovery (green) reach in h2 h2 -> 2j 3l + met channel at the HL-LHC.

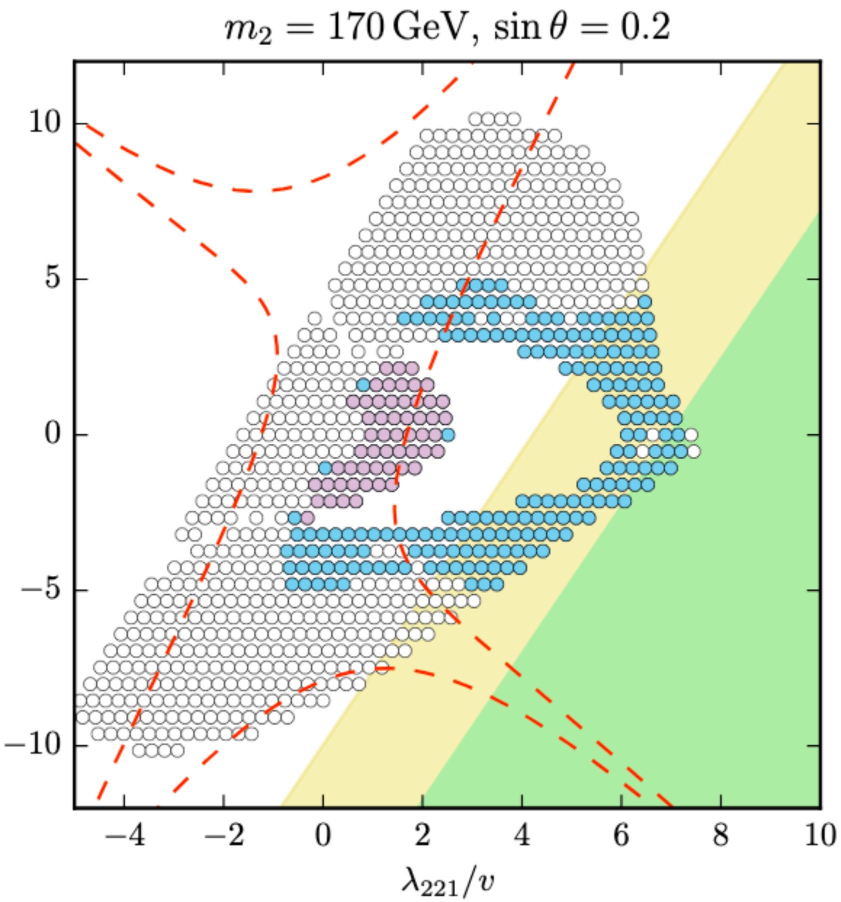

Exclusion (yellow) reach in h1 h2 + h1 h1 -> bb 2l + met channel at the HL-LHC.

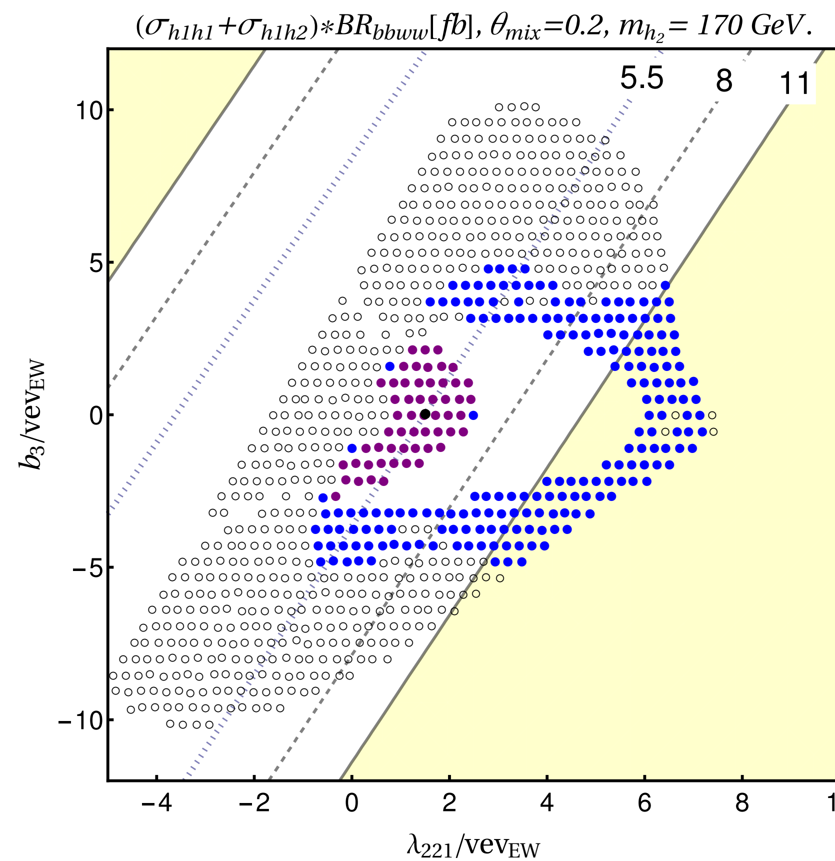

Blue points feature an EWPT with $\phi_h(T_c)/T_c \geq 1$ for some value of $b_4 > 0.01$ utilizing the one-loop daisy-resummed thermal effective potential. Purple points additionally feature a strong first-order electroweak phase transition as predicted by the gauge-invariant high-T approximation (which drops the Coleman-Weinberg potential and is thus only applied to regions with tree-level vacuum stability). Strong electroweak phase transitions are typically correlated with sizable values of λ_{221}.

Summary

- Higgs self couplings are important to understand the nature of electroweak symmetry breaking. The HL-LHC will have a sensitivity to the measurement of the triple Higgs coupling via double Higgs production, and it is a guaranteed physics.
- Double Higgs production is challenging due to small signal cross section / large SM backgrounds, which requires combination of multiple channels.
- bbWW dilepton channel is one of the most difficult channels due to strong correlation among many kinematic variables.
- Multivariate analysis could benefit from deep neural networks using jet images and sophisticated kinematic variables such as Topness / Higgsness with mass information. Further improvement may be possible by optimizing network structure (ResNets, CapsNets)
- bbWW channel could make a significant contribution in the combination of multiple channels for the triple Higgs coupling measurement.
- Semi-leptonic channel would be similar.